Molecular Therapy
Original Article

Inhibition of adenylyl cyclase 8 prevents the upregulation of Orai1 channel, which improves cardiac function after myocardial infarction

Débora Falcón,[1,2] Eva M. Calderón-Sánchez,[1,2] Isabel Mayoral-González,[1] Marta Martín-Bórnez,[1,2] Alejandro Dominguez-Rodriguez,[1] Encarnación Gutiérrez-Carretero,[1,3] Antonio Ordóñez-Fernández,[1] Juan Antonio Rosado,[4,5] and Tarik Smani[1,2,5]

[1]Group of Cardiovascular Pathophysiology, Institute of Biomedicine of Seville, University Hospital of Virgen del Rocio/University of Seville/CSIC, 41013 Seville, Spain; [2]Department of Medical Physiology and Biophysics, Faculty of Medicine, University of Seville, 41009 Seville, Spain; [3]Department of Surgery, Faculty of Medicine, University of Seville, 41009 Seville, Spain; [4]Department of Physiology, Institute of Molecular Pathology Biomarkers, University of Extremadura, 10003 Caceres, Spain

The upregulation of Orai1 and subsequent store-operated Ca^{2+} entry (SOCE) has been associated with adverse cardiac remodeling and heart failure (HF). However, the mechanism underlying Orai1 upregulation and its role in myocardial infarction remains unclear. Our study investigated the role of Orai1 in activating adenylyl cyclase 8 (AC8) and cyclic AMP (cAMP) response element-binding protein (CREB), as well as its contribution to cardiac dysfunction induced by ischemia and reperfusion (I/R). We found that I/R evoked an increase in the expression of Orai1 and AC8 in rats' hearts, resulting in a substantial rise in diastolic Ca^{2+} concentration ($[Ca^{2+}]_i$), and reduced ventricular contractions. The expression of Orai1 and AC8 was also increased in ventricular biopsies of post-ischemic HF patients. Mechanistically, we demonstrate that I/R activation of Orai1 stimulated AC8, which produced cAMP and phosphorylated CREB. Subsequently, *p*-CREB activated the *ORAI1* promoter, resulting in Orai1 upregulation and SOCE exacerbation. Intramyocardial administration of AAV9 carrying AC8 short hairpin RNA decreased the expression of AC8, Orai1 and CREB, which restored diastolic $[Ca^{2+}]_i$ and improved cardiac contraction. Therefore, our data suggests that the axis composed by Orai1/AC8/CREB plays a critical role in I/R-induced cardiac dysfunction, representing a potential new therapeutic target to limit the progression of the disease toward HF.

INTRODUCTION

According to the World Health Organization acute myocardial infarction (AMI) remains the leading cause of mortality worldwide (https://www.who.int/es/news-room/fact-sheets/detail/the-top-10-causes-of-death). Reperfusion therapeutic strategies, such as primary angioplasty or pharmacological thrombolytic treatments, have effectively decreased the mortality rates associated with AMI. However, despite their need for heart salvage, reperfusion therapies produce detrimental intracellular signals, causing additional damage to the vulnerable heart. This phenomenon is known as ischemia and reperfusion (I/R) syndrome, which contributes to the adverse cardiac remodeling and its progression toward heart failure (HF).[1,2]

Cardiac dysfunction during pathological heart remodeling is associated with changes in the expression and activity of Ca^{2+}-related proteins, such as ion channels, Ca^{2+}-ATPase pumps, and Na^+/Ca^{2+} exchanger.[3,4] In the past decade, Orai1-mediated store-operated Ca^{2+} entry (SOCE) has been shown to play a role in cardiovascular remodeling associated with various etiologies, including transverse aortic constriction, pulmonary arterial hypertension, and myocardial infarction.[5–7] SOCE is typically initiated because of a decrease in Ca^{2+} levels in the endoplasmic and sarcoplasmic reticulum lumen, which activates the interaction of Ca^{2+} sensing STIM proteins with Orai1 channels, resulting in Ca^{2+} influx and a sustained increase in the intracellular concentration of Ca^{2+} ($[Ca^{2+}]_i$), ultimately leading to the activation of various signal transduction pathways.[6] Significant overexpression of Orai1 was observed in cardiac myocytes isolated from the rat model of I/R, resulting in an exacerbated SOCE.[8] However, the role of Orai1 in the pathophysiological downstream signaling pathways in the heart under I/R remains barely studied. There is growing evidence indicating that Orai1 activates transcription factors, like the nuclear factor of activated T cells (NFATs), the nuclear factor κ-light chain-enhancer of activated B cells, and the cyclic AMP (cAMP) response element-binding (CREB) in both excitable and non-excitable cells.[9] In the heart, the activation of NFAT by Orai1 and SOCE has been associated with the induction of pro-hypertrophic genes, resulting in pathological cardiac remodeling and

Received 24 August 2023; accepted 19 January 2024;
https://doi.org/10.1016/j.ymthe.2024.01.026.

[5]These authors contributed equally

Correspondence: Débora Falcón, Instituto de Biomedicina de Sevilla (IBiS), Calle Antonio Maura S/N, Sevilla 41013, Spain.
E-mail: dfalcon-ibis@us.es
Correspondence: Tarik Smani, Instituto de Biomedicina de Sevilla (IBiS), Calle Antonio Maura S/N, Sevilla 41013, Spain.
E-mail: tasmani@us.es

Please cite this article in press as: Falcón et al., Inhibition of adenylyl cyclase 8 prevents the upregulation of Orai1 channel, which improves cardiac function after myocardial infarction, Molecular Therapy (2024), https://doi.org/10.1016/j.ymthe.2024.01.026

dysfunction.[10,11] Meanwhile, CREB is a well-studied target of both Ca^{2+} and cAMP signaling in various cell types, including neurons and vascular smooth muscle cells.[12] However, as far as we know, the impact of CREB activation by SOCE on the heart has not yet been addressed.

Independent studies have shown that Orai1α, the longer form of Orai1, contains an interacting sequence with Ca^{2+}-sensitive adenylyl cyclase 8 (AC8) (residues 23−34),[13] and Ca^{2+} influx through Orai1 stimulated AC8 which promoted the production of cAMP and subsequent activation of protein kinase A (PKA) in HEK293 and triple negative breast cancer cells.[14,15] In addition, the activation of AC8 promotes cAMP stimulation of various regulatory proteins like phosphodiesterase, PKA, protein kinase C, and calcineurin, which are all associated with cardiac pathophysiology signaling pathways, involving fibrosis and hypertrophy.[16] However, the effect of Orai1 activation on AC8 and cAMP/CREB signaling under AMI remains unexplored. In the present study, we examined the role of Orai1 in I/R-induced $[Ca^{2+}]_i$ dysregulation and evaluated the involvement of AC8, cAMP, and CREB in cardiac dysfunction. Our findings reveal that Orai1, AC8, and CREB form an axis, whose activation is crucial for I/R-induced cardiac remodeling associated with Orai1 overexpression, suggesting that pharmacological inhibition of this axis may provide a novel therapeutic strategy to alleviate post-infarction adverse remodeling and limit the development of HF.

RESULTS

I/R induces cardiac dysfunction, which is associated with an increase in diastolic $[Ca^{2+}]_i$ due to SOCE activation

Figure 1A shows that I/R induces a significant decrease in cardiac contractile capacity as examined by M-mode echocardiography after 1 week of the intervention, following the protocol described in Figure S1A. Figure 1B confirms significant decreases in the left ventricular fractional shortening (LVFS) in I/R group, as compared with sham, indicating that heart contraction is significantly affected after I/R. Given the crucial role played by Ca^{2+} in regulating heart contractility, we evaluated the changes in the $[Ca^{2+}]_i$ induced by field stimulation at 0.5 Hz. As depicted in Figures 1C and 1D, I/R significantly reduces both $[Ca^{2+}]_i$ responses and cell shortening, as demonstrated by the representative line-scan Ca^{2+} images of adult rat ventricular myocytes (ARVMs) isolated from sham and I/R rats. Figures 1E and 1F confirm significant decreases in the amplitude of $[Ca^{2+}]_i$ transients recorded in ARVMs isolated from I/R rats, compared with sham. Additionally, Figure 1G shows that $[Ca^{2+}]_i$ transient decay time is significantly increased in AVRM from I/R rats when compared with sham. Figure 1H also shows that I/R significantly increases the resting level of $[Ca^{2+}]_i$, (F_0), before cell stimulation, indicating a mishandling of diastolic $[Ca^{2+}]_i$ in I/R conditions. To corroborate this observation, we conducted ratiometric analysis on Fura-2-loaded cells. As illustrated in Figures 1I and 1J, the diastolic $[Ca^{2+}]_i$ is significantly enhanced in field-stimulated ARVM isolated from I/R rat, as compared with those isolated from sham. This increase could be due to the activation of different molecular players involved in Ca^{2+} homeostasis. Therefore, we analyzed the phosphorylation profile of ryanodine receptor 2 (RyR2) and observed that I/R induces RyR2 phosphorylation at Ser^{2030} in heart tissue (Figure 1K).

Previous studies have shown that SOCE and related proteins are also involved in the increased diastolic $[Ca^{2+}]_i$ in cardiac myocytes treated with aldosterone,[17] as well as in ARVM of transgenic mice overexpressing STIM1.[18] Therefore, we investigated if SOCE participates in I/R-induced diastolic $[Ca^{2+}]_i$ elevation. As shown in Figures 1I and 1J, the preincubation of ARVM of I/R rats with 10 μM GSK-7975A, a widely used store operated Ca^{2+} channel inhibitor,[19] significantly prevents the increase in diastolic $[Ca^{2+}]_i$. Similarly, Figure S2 shows that electric field stimulation of neonatal rat ventricle myocytes (NRVMs) at 1 Hz under an I/R protocol (Figure S1C) elicits a substantial increase in the diastolic $[Ca^{2+}]_i$, which is significantly inhibited in cells pre-incubated with SYNTA-66 (20 μM), another SOCE inhibitor.[20] These findings indicate that the increase in diastolic $[Ca^{2+}]_i$ induced by I/R involves the activation of SOCE.

I/R exacerbates SOCE through Orai1 upregulation

Orai1 is the main isoform responsible for SOCE in many cells, including cardiac myocytes.[5,8] As shown in Figures 2A and 2B, the expression of Orai1 protein in rat's heart and NRVM is significantly increased by I/R. Therefore, to evaluate the role of Orai1 in $[Ca^{2+}]_i$ handling under I/R, we examined the effect of Orai1 downregulation on SOCE in NRVM, using small interfering RNA (siRNA). Figure 2C confirms that siRNA of Orai1 (siOrai1) successfully reduced its expression in NRVM. Next, we performed the classical Ca^{2+} add-back protocol for SOCE activation by incubating NRVM with thapsigargin (TG, 2 μM) in the presence of nifedipine (1 μM), to inhibit L-type Ca^{2+} channels, for 10 min. As illustrated in Figures 2D and 2E, TG induces a significant increase in the $[Ca^{2+}]_i$ after Ca^{2+} restoration in NRVMs subjected to I/R, as compared with control cells and to those transfected with scramble (data not shown). Meanwhile, Orai1 inhibition by siOrai1 prevents the effect of TG, confirming the implication of Orai1 in I/R induced-exacerbated SOCE.

I/R stimulates AC8 and cAMP production by Orai1-dependent SOCE

The functional relationship between Orai1 and different proteins has been described previously in many cell types. In this study, we explored the functional interaction between AC8 and Orai1 and investigated the expression of AC8 under I/R. As depicted in Figure 3A, the expression of AC8 is significantly increased in the adult heart and in NRVM after I/R. Given that AC8 is a Ca^{2+}-sensitive isoform that catalyzes the formation of cAMP from ATP, we examined whether SOCE activates AC8 during I/R, by assessing cAMP production in NRVM. Figure 3B shows a significant increase in cAMP levels in NRVMs exposed to reperfusion after ischemia, as compared with control NRVMs. In contrast, cells treated with GSK-7975A (10 μM), an Orai1 inhibitor, effectively prevents I/R-induced increase of cAMP levels. To demonstrate the role of AC8 in cAMP production under I/R, we performed similar experiments in NRVM, wherein AC8 was successfully downregulated by siRNA (siAC8), as confirmed

Please cite this article in press as: Falcón et al., Inhibition of adenylyl cyclase 8 prevents the upregulation of Orai1 channel, which improves cardiac function after myocardial infarction, Molecular Therapy (2024), https://doi.org/10.1016/j.ymthe.2024.01.026

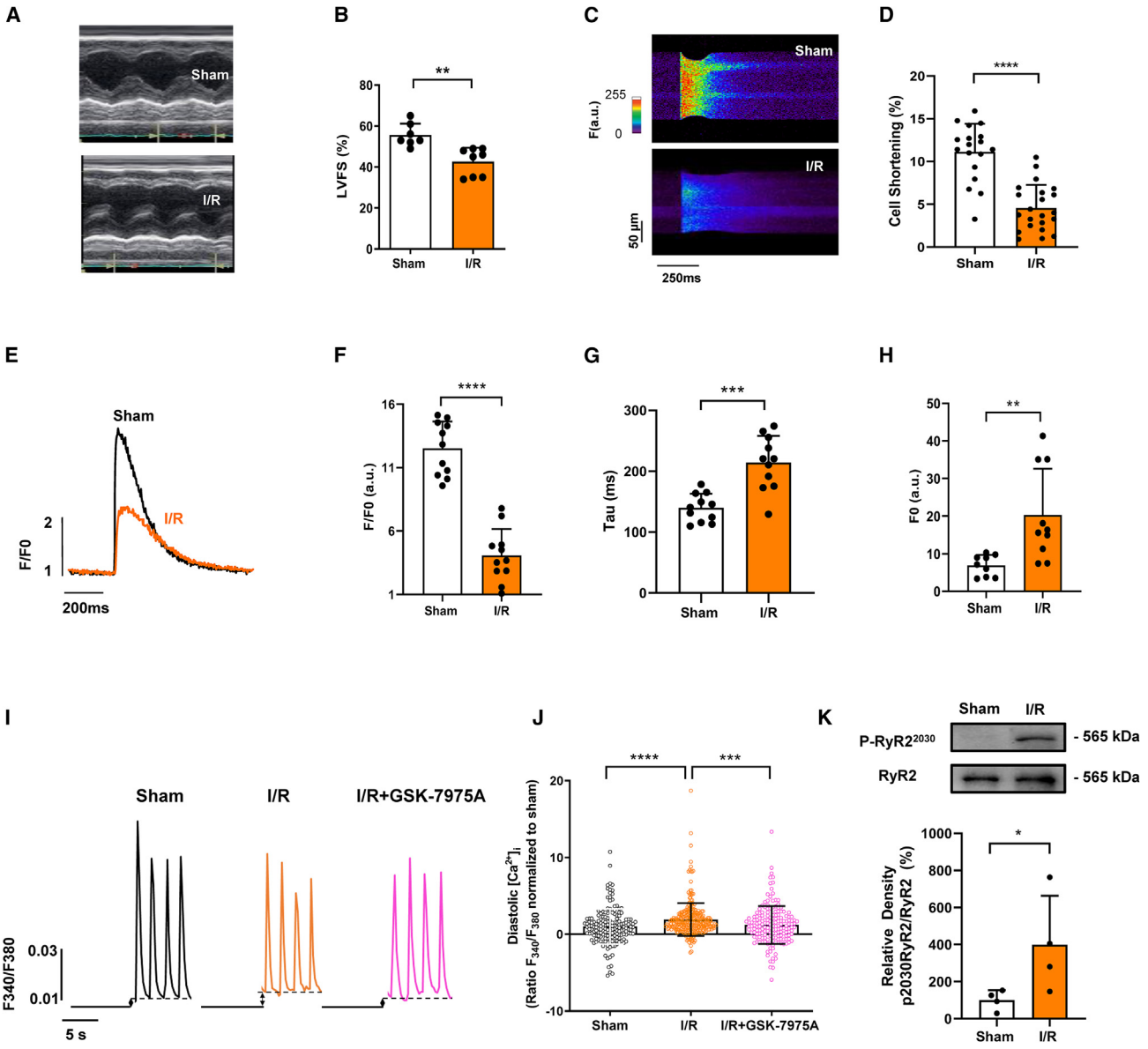

Figure 1. I/R evokes cardiac dysfunction associated with an increase in the diastolic $[Ca^{2+}]_i$ due to the activation of SOCE

(A) Representative M-mode echocardiographic images evaluated 1 week after the intervention in sham and I/R rats. (B) Bar graph shows LVFS (%) measured in sham and I/R rats. n = 7–8 rats/condition. (C) Representative line-scan images during field stimulation at 1 Hz of cardiac myocytes isolated from "sham" and "I/R" rats. (D) Bar graph shows cellular shortening expressed in percentage of cell length in "sham" and "I/R." n = 18–22 cells from 3 rats/condition. (E) Representative $[Ca^{2+}]_i$ transients and bar graphs showing mean values of (F) the amplitude of $[Ca^{2+}]_i$ transient measured as the peak of F/F_0, where F is the fluorescence and F_0 is the fluorescence in the diastolic period, (G) Decay constant time (tau), and (H) intracellular resting $[Ca^{2+}]_i$ recorded in Fluo-3AM loaded cardiac myocyte isolated from "sham" and "I/R" rats. n = 9–11 cells from 3 rats/condition. (I) Representative $[Ca^{2+}]_i$ transients and (J) summary data of diastolic $[Ca^{2+}]_i$ normalized to values in sham recorded as Fura-2 ratio (F340/F380) in 0.5 Hz field stimulated cardiac myocyte isolated from "sham" and "I/R" rats, 1 week after surgery. "I/R+GSK-7975A" indicates cardiac myocyte isolated from I/R rats and pre-incubated for 5 min with 10 μM GSK-7975A, before their stimulation. n = 250–290 cells from 4 to 5 rats/condition. (K) Representative immunoblots (top) and summary data (bottom) showing protein ratio of *p*-RyR2^{2030} related to RyR2. Samples are from heart tissues of "sham" and I/R rats, assessed 1 week after the intervention. n = 4 rats/condition. Data are expressed as means ± SD. *,**,***, and **** indicate significance at $p < 0.05$, $p < 0.01$, $p < 0.001$ and $p < 0.0001$, respectively.

in Figure S3. We found that siAC8 significantly inhibits I/R-induced cAMP (Figure 3B), indicating that I/R stimulates cAMP synthesis via AC8 and Orai1 activation in NRVMs.

To further investigate the physical interaction of Orai1 and AC8, we used immunofluorescence staining to explore the endogenous localizations of Orai1 and AC8 in NRVMs exposed to I/R and

Please cite this article in press as: Falcón et al., Inhibition of adenylyl cyclase 8 prevents the upregulation of Orai1 channel, which improves cardiac function after myocardial infarction, Molecular Therapy (2024), https://doi.org/10.1016/j.ymthe.2024.01.026

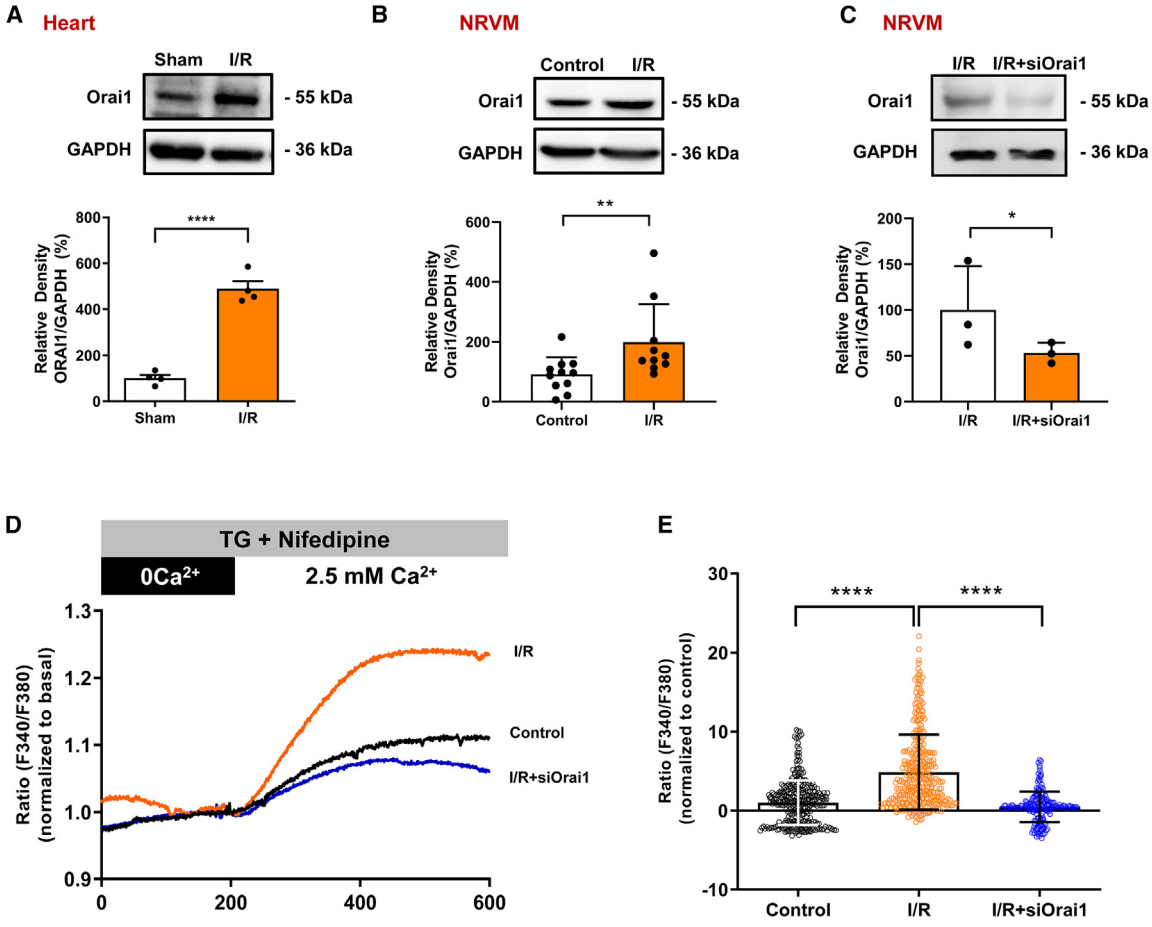

Figure 2. I/R stimulates Orai1 upregulation and an exacerbated SOCE

Representative immunoblots (top) and summary data (bottom) of Orai1 protein normalized to its corresponding GAPDH.

(A) Data are from heart tissues of "sham" and "I/R" rats, assessed 1 week after the intervention (n = 4 rats/condition). (B) Samples were from untreated NRVM "Control" and from NRVM subjected to "I/R." (C) Samples were from "I/R" NRVM, and from I/R NRVM transfected with siRNA to inhibit Orai1 "I/R + siOrai1." Mean values are from n = 3–10 independent cultures. (D) Representative traces and (E) mean values of TG-induced Ca^{2+} influx in Fura-2 loaded NRVMs. Cells were pre-incubated with 2 μM TG in presence of 1 μM nifedipine to inhibit L-type Ca^{2+} channels. Recordings are from "Control" NRVM, from NRVM subjected to "I/R," and from "I/R" NRVM transfected with siOrai, "I/R + siOrai1" (n = 190–350 cells from 5 cultures). "I/R" in NRVM corresponds to 3 h of ischemia and followed by 72 h of reperfusion. Data are expressed as means ± SD. *, **, and ****indicate significance at $p < 0.05$, $p < 0.01$ and $p < 0.0001$, respectively.

in section of rat's heart. Merge images in Figure 3C shows a detectable co-localization of AC8 and Orai1 in control NRVM, which significantly increases after their exposition to I/R for 5 min, as confirmed by Pearson's correlation coefficient (PCC) analysis (Figure 3D). Similarly, images from hearts show a low basal interaction of Orai1 and AC8 in sham group, which increases significantly in the infarcted area 1 week after I/R (Figure 3E), as confirmed by PCC (Figure 3F). These results demonstrate significant overlap of Orai1 and AC8 staining in cardiac myocytes and heart under I/R.

I/R induces CREB phosphorylation through PKA activation

To investigate the downstream pathways involved in I/R-mediated stimulation of Orai1 and AC8, we focused on the potential activation of the transcription factor CREB, which can be activated both by Ca^{2+} and cAMP signaling, as reviewed elsewhere.[21] Immunostaining images in Figure 4A confirm CREB activation in the nuclei of NRVM exposed for 5 min to reperfusion, while no activation was observed after 30 min of I/R. The activation of CREB is confirmed by western blotting in NRVMs, 5 min after reperfusion, as assessed by CREB Ser133 phosphorylation (Figure 4B). However, CREB activation is decreased within 30 min of reperfusion and completely lost 24 h after cell stimulation with I/R. Similarly, Figure 4C shows that the exposition of ARVMs for 5 min to I/R-induced CREB phosphorylation. Moreover, we analyzed the implication of PKA, ERK1/2, and Epac2 in CREB phosphorylation, by using specific inhibitors, namely H89 (1 μM), PD98059 (5 μM), and ESI-05 (10 μM), respectively. As depicted in Figures 4C and 4D, only H89 significantly reduces I/R-mediated CREB activation, while ERK1/2 and EPAC2 have no apparent role in this activation. Furthermore, the western blot experiment in

Please cite this article in press as: Falcón et al., Inhibition of adenylyl cyclase 8 prevents the upregulation of Orai1 channel, which improves cardiac function after myocardial infarction, Molecular Therapy (2024), https://doi.org/10.1016/j.ymthe.2024.01.026

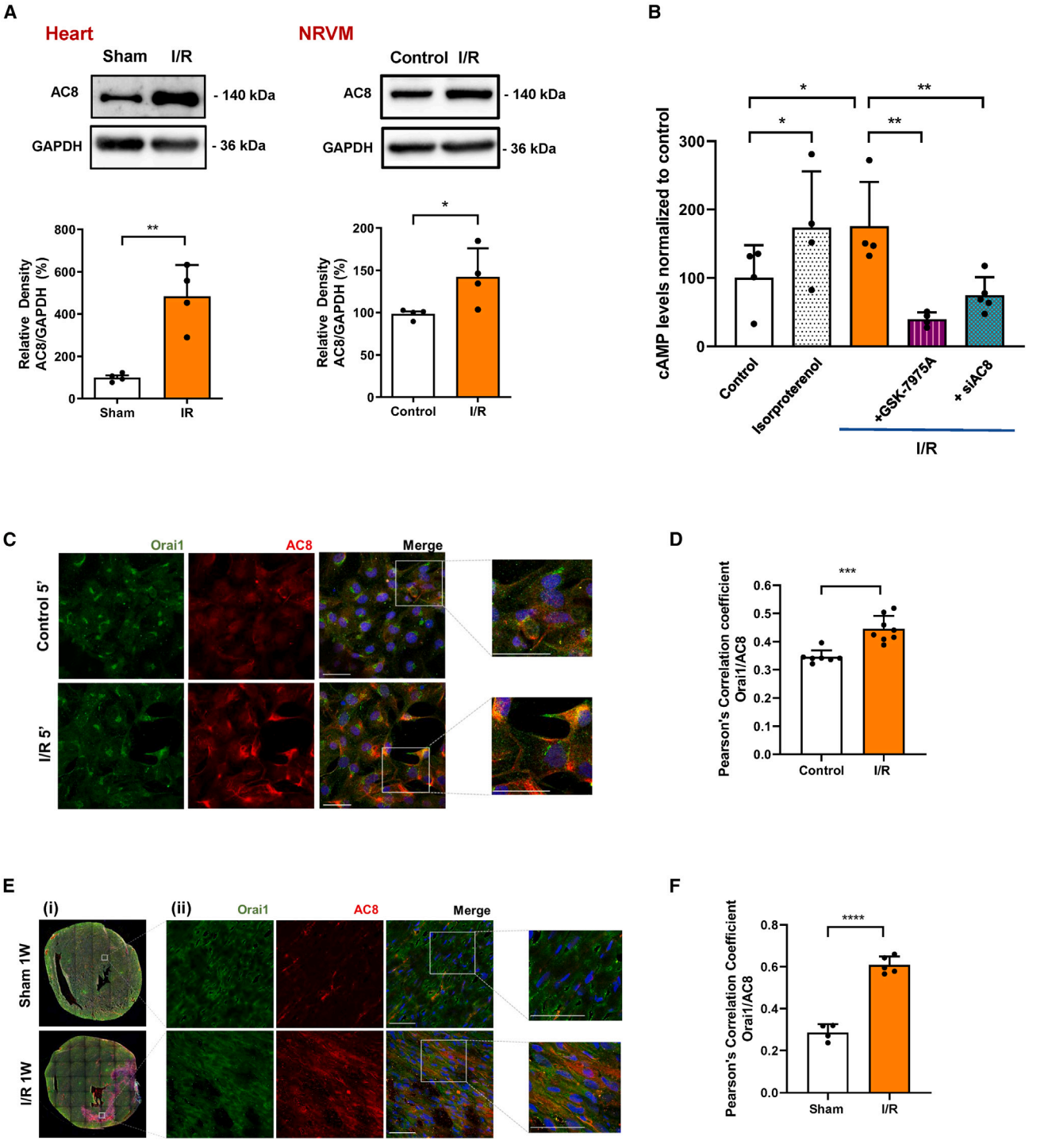

Figure 3. I/R increases AC8 expression and stimulates its co-localization with Orai1

(A) Representative immunoblots (top) and summary data (bottom) of protein expression of AC8 normalized to their corresponding GAPDH. In left panel, samples were from heart tissues of "sham" and "I/R" rats, examined 1 week after the intervention (n = 4 rats/condition). In right panel, samples were from "Control" NRVM, and NRVM subjected to "I/R" (3 h of ischemia and followed by 72 h of reperfusion). n = 4 independent cultures. (B) Bar graph showing cAMP levels in untreated NRVM "Control"; NRVM treated with 1 μM isoproterenol to stimulate cAMP production through beta-adrenergic receptors; "I/R" NRVM exposed to reperfusion after ischemia; NRVM pre-incubated with 10 μM GSK-7975A before I/R "+GSK-7975A"; and NRVM transfected with siRNA of AC8 "+siAC8" and exposed to I/R. n = 4 independent cultures. I/R protocol corresponds 3 h of

(legend continued on next page)

Please cite this article in press as: Falcón et al., Inhibition of adenylyl cyclase 8 prevents the upregulation of Orai1 channel, which improves cardiac function after myocardial infarction, Molecular Therapy (2024), https://doi.org/10.1016/j.ymthe.2024.01.026

Figure 4B confirms that NRVM pre-incubation with H89 inhibits I/R induced-CREB phosphorylation.

The activation of CREB and AC8 is required for Orai1 upregulation during I/R

Considering that I/R stimulates CREB and it also increases Orai1 expression, we investigated whether CREB plays a role in I/R-induced Orai1 overexpression that leads to SOCE potentiation. In silico analysis using MatInspector software (Genomatix, GE) identified compatible sequences with CREB-responsive elements in a region of approximately 3,000 bp upstream of the coding sequence of rat *ORAI1* gene (Figure S4A). Next, we used 666-15, a cell-permeable inhibitor of CREB,[22] to explore if CREB transcribes Orai1 expression. First, western blotting and immunostaining in Figures 5A and 5B confirm that NRVM pre-incubation with 666-15 (3 μM) inhibits CREB phosphorylation under I/R. Second, as illustrated in Figure 5C, 666-15 inhibits I/R-induced Orai1 overexpression in NRVM, as compared with untreated I/R cells. It also significantly inhibits TG-evoked SOCE potentiation under I/R (Figures 5D and 5E), demonstrating that CREB activation is involved in the upregulation of Orai1 and subsequent exacerbated SOCE induced by I/R.

To further investigate how CREB regulates the expression of Orai1, the A7r5 cell line was transiently transfected with a reporter gene plasmid containing the rat *ORAI1*-promoter driving the firefly luciferase gene, and then exposed to TG (2 μM) to induce SOCE. First, Figure S4B confirms that TG (2 μM) activates CREB in A7r5 which is inhibited by 666-15 (3 μM). Second, as shown in Figure 5F, TG increases *ORAI1* transcriptional activity as demonstrated by the significantly enhanced luciferase activity. Interestingly, cells before incubation with 666-15 (3 μM) block the effect of TG, confirming that CREB activation is required for TG-induced *ORAI1* transcription. Additionally, cells before treatment with GSK-7975A (10 μM) inhibits TG-induced luciferase activity, suggesting that Ca^{2+} entry through Orai1 is necessary for its own transcription.

Considering the previous findings showing that AC8 is upstream I/R activation of CREB, we investigated whether AC8 activation is necessary for Orai1 expression and exacerbation of SOCE under I/R. As depicted in Figures 5G and 5H, silencing of AC8 prevents TG-induced SOCE increase in NRVM under I/R. Additionally, Figures 5I and S5 demonstrate that adeno-associated virus serotype 9 (AAV9) carrying AC8 short hairpin RNA (shRNA) (AAV9-AC8) efficiently inhibits I/R-induced upregulation of Orai1 in NRVM.

Altogether, these data demonstrate that Orai1-dependent SOCE induced by I/R activates AC8, which subsequently activates CREB. This activation is required for I/R-induced Orai1 upregulation and SOCE potentiation, suggesting a positive feedback loop within this signaling pathway.

In vivo administration of AAV9-AC8 reduces Orai1 expression and improves cardiac function after I/R

In view of these results, we investigated whether the activation of AC8, CREB, and Orai1 is relevant for $[Ca^{2+}]_i$ mishandling and cardiac dysfunction under I/R. Therefore, we performed *in vivo* experiments using intramyocardial injection of AAV9-AC8. Figures 6A and 6B show that AAV9-AC8 potently inhibits I/R-induced overexpression of AC8, Orai1, CREB, and *p*-CREB in rat hearts. Interestingly, as illustrated in Figures 6C and 6D, diastolic $[Ca^{2+}]_i$ is restored to basal levels in ARVMs isolated from the heart of AAV9-AC8 rats 1 week after the intervention, confirming the involvement of AC8 in diastolic $[Ca^{2+}]_i$ alteration, certainly via Orai1, as shown earlier in Figure 5I.

To elucidate the relationship between the activation of AC8 by Orai1 and cardiac dysfunction, we used the speckle tracking echocardiography analysis to examine cardiac function *in vivo* in rats after 1 and 4 weeks of the intervention. As shown by representative images in Figure 7A and summarized in Figures 7B–7D, the peak systolic circumferential strain (PSCS), the global circumferential strain (GCS), and the global radial strain (GRS) examined at the papillary muscle are markedly decreased in the I/R group, as compared with sham. The decrease in these parameters persisted 1 week after the administration of AAV9-AC8. In contrast, PSCS, GCS, and GRS recovered significantly when examined 4 weeks after the intervention in the same rats. Similarly, longitudinal strain is significantly decreased in I/R rats and trends to recover in AAV9-AC8 transfected rats (Figures S6A and S6B). Furthermore, conventional echocardiographic analysis shows that LVFS is significantly restored after AAV9-AC8 injection in I/R rats 4 weeks after surgery (Figure S6C). These results confirm that AC8 downregulation mitigates cardiac dysfunction in I/R conditions.

The myocardium of post-ischemic HF patients exhibits high levels of Orai1 and AC8

To extend the previous main results to the failing human heart, we analyzed the expression of Orai1, AC8, and CREB in heart biopsies obtained from patients with ischemic HF and compared them with those from healthy biopsies (unused from non-HF transplant donors). As shown in Figures 8A and 8B, Orai1 and AC8 are significantly overexpressed in HF patients as compared with healthy biopsies, while

ischemia followed by 2 min of reperfusion. (C) Representative images of immunofluorescence showing Orai1 (green) and AC8 (red) staining in NRVM in "control" and "I/R" conditions. I/R corresponds with 3 h of ischemia and followed by 5 min of reperfusion. Images were taken with a 63× objective in the same z-position; scale bar, 40 μm; n = 8 images from three independent cultures. (E) Representative images of immunofluorescence showing Orai1 (green) and AC8 (red) staining in heart from "sham" and "I/R" rats, 1 week after surgery. (i) Images of section of heart taken with a 10× objective in the same z-position. (ii) Images of heart's tissue taken with a 63× objective in the same z-position; scale bar, 40 μm; n = 4–5 rats/condition. Yellow color in the merge images and (D) and (F) means value of PCC indicating Orai1 and AC8 co-localization in similar experiments as in (C) and (E). Nuclei were stained in blue. Data are expressed as means ± SD. *, **, ***, and **** indicate significance at $p < 0.05$, $p < 0.01$, $p < 0.001$ and $p < 0.0001$, respectively.

Please cite this article in press as: Falcón et al., Inhibition of adenylyl cyclase 8 prevents the upregulation of Orai1 channel, which improves cardiac function after myocardial infarction, Molecular Therapy (2024), https://doi.org/10.1016/j.ymthe.2024.01.026

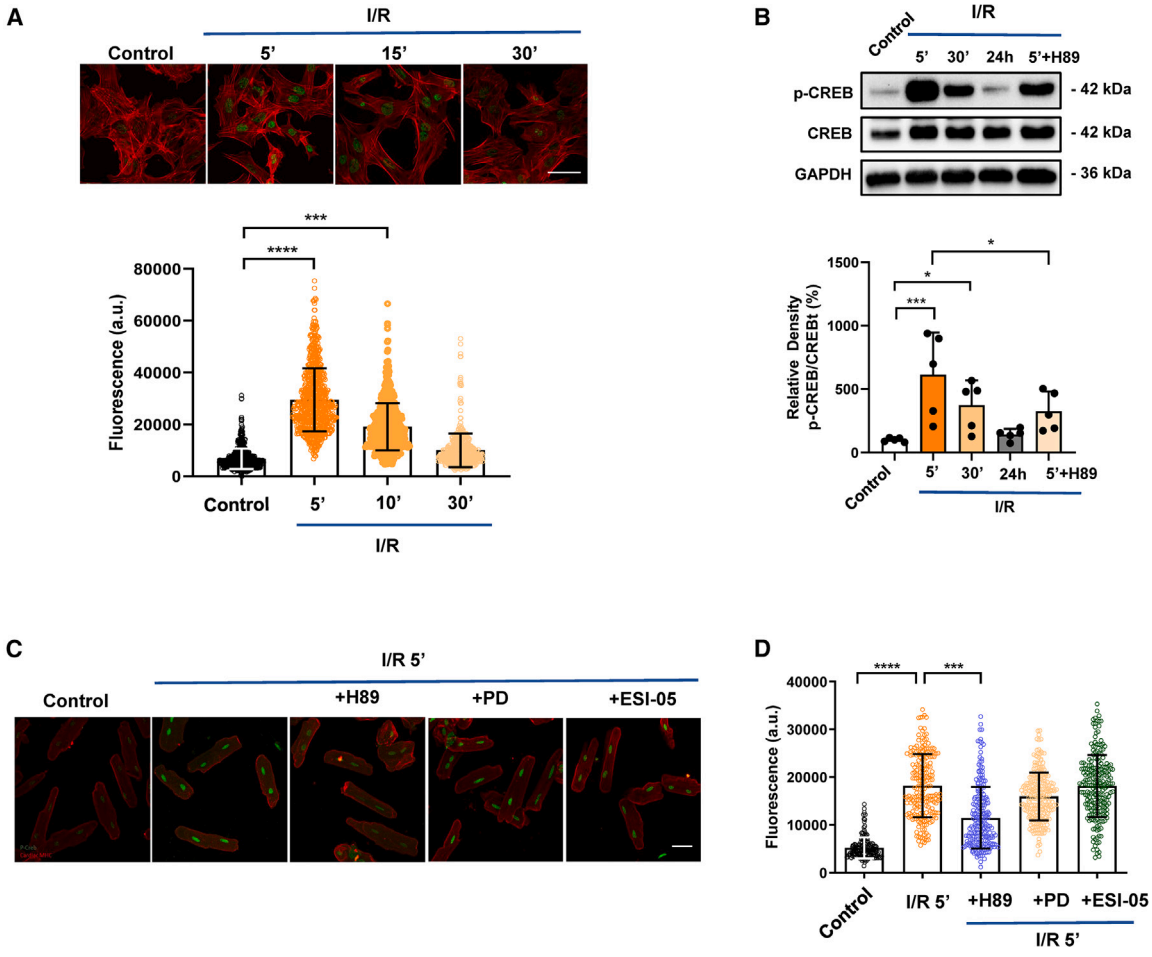

Figure 4. I/R activates cAMP response element-binding

(A) Representative images (top) and summary data (bottom) showing CREB phosphorylation (green) and F-actin stained with phalloidin (red) detected by immunofluorescence in "Control" NRVMs, and in NRVMs exposed 5, 15, and 30 min to reperfusion after 3 h of ischemia. Scale bar, 5 μm; n = 100–160 cells from four independent cultures. (B) Representative western blots (top) and summary data (bottom) showing protein density of *p*-CREB related to CREB total (CREBt). Samples are from "Control" NRVMs; from NRVMs exposed 5 and 30 min, and 24 h to reperfusion after ischemia; and from NRVMs pre-incubated with 1 μM H89 and exposed 5 min to I/R. n = 5 independent cultures. Representative immunofluorescence images (C) of AVRM and summary data (D) showing CREB phosphorylation (green) and beta myosin heavy chain (red). Scale bar, 30 μm. AVRM were exposed 5 min to reperfusion after 40 min of ischemia (I/R), pre-incubated with 1 μM H89, 5 μM PD98059 (+PD), and 10 μM ESI-05 (+ESI-05), to inhibit PKA, ERK1/2, and Epac2, respectively. n = 170–200 cells from three independent cultures. Data are expressed as means ± SD. *, ***, and **** indicate significance at $p < 0.05$, $p < 0.001$ and $p < 0.0001$, respectively.

Figure 8C shows only a tendency of CREB overexpression in HF. In accordance with the western blotting results (Figures 8A and 8B), immunofluorescence analysis in Figure 8D and the movies in Supplemental data (Video S1 and Video S2) show an increased detection of Orai1 and AC8 in histological sections from HF compared with non-HF myocardia. These findings demonstrate significant increase in Orai1 and AC8 expression in post-infarction HF patients, which may be associated with decreased cardiac function.

DISCUSSION

The current study revealed a novel mechanism which is centered on Orai1 activation of AC8, and CREB transcription of Orai1 itself forming a positive feedback loop contributing to cardiac dysfunction after I/R, as summarized in Figure S7. We have used a combination of *in vivo* and *in vitro* approaches to demonstrate for the first time that Ca^{2+} entry through Orai1 stimulates AC8 under I/R, which activates the CREB through PKA pathway. This activation regulates Orai1 expression, resulting in a mishandling of Ca^{2+} homeostasis that is associated with an increase in diastolic $[Ca^{2+}]_i$ and exacerbated SOCE. Moreover, AC8 inhibition with AAV9-AC8 prevents I/R-induced Orai1 overexpression and significantly improves cardiac hemodynamic parameters. Thus, we have identified an unexpected positive feedback loop formed by Orai1/AC8/CREB/Orai1 that regulates Orai1 expression under I/R, suggesting that the activation of this loop could potentially compromise myocardial function in AMI patients.

Please cite this article in press as: Falcón et al., Inhibition of adenylyl cyclase 8 prevents the upregulation of Orai1 channel, which improves cardiac function after myocardial infarction, Molecular Therapy (2024), https://doi.org/10.1016/j.ymthe.2024.01.026

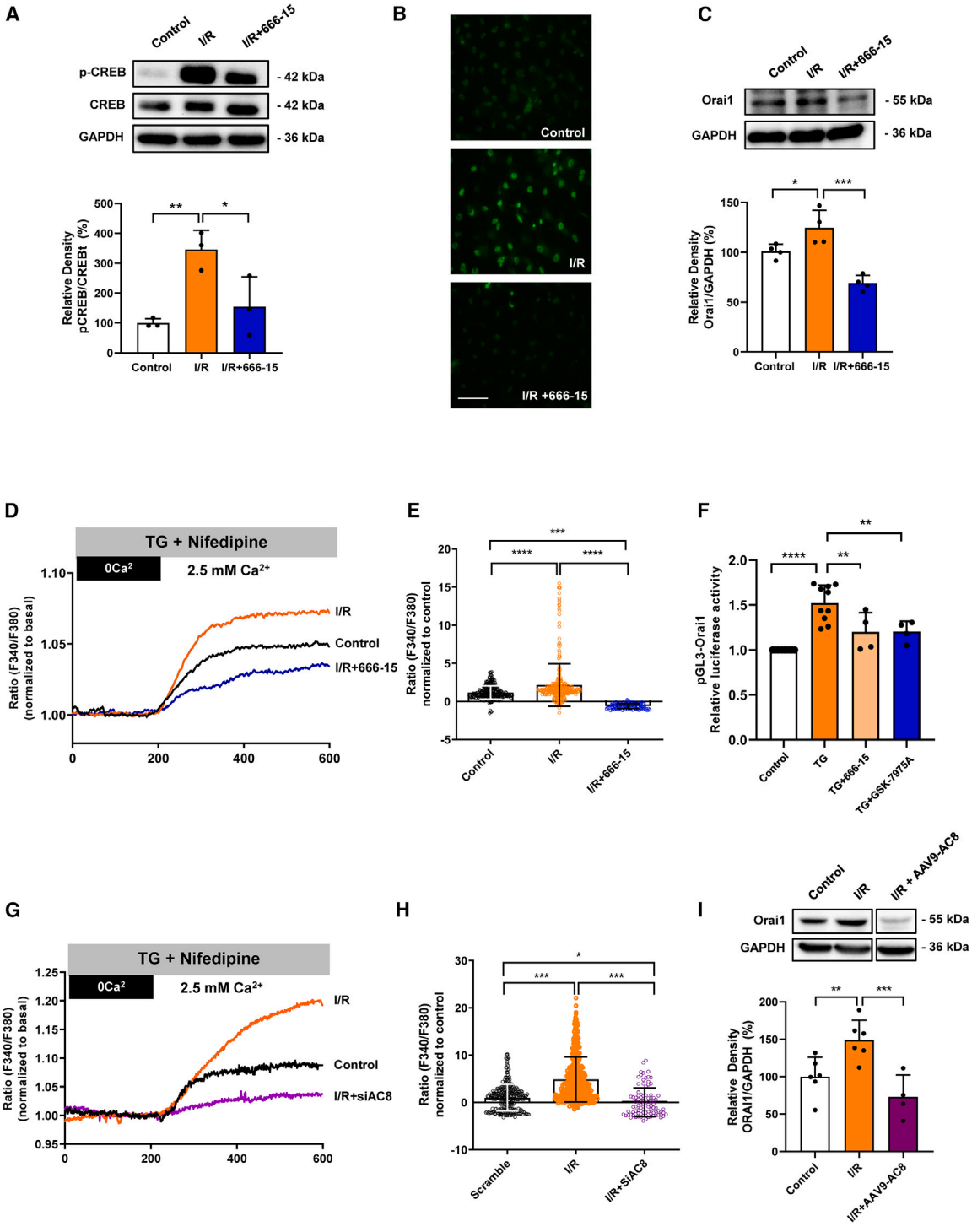

Figure 5. I/R-induced CREB activation regulates Orai1 expression

(A) Immunoblots (top) and summary data (bottom) of *p*-CREB related to CREB total (CREBt). Samples were from "Control" NRVMs; NRVMs exposed 5 min to reperfusion after 3 h of ischemia "I/R"; and "I/R" NRVMs pre-incubated 3 h with 3 μM 666-15 "I/R+6665-15." n = 3 independent cultures. (B) Representative images of experiments as in (A) showing CREB phosphorylation in NRVM (green) using immunofluorescence. Scale bar, 10 μm. (C) Immunoblots (top) and summary data (bottom) of Orai1 expression normalized to its corresponding GAPDH examined in "Control" NRVMs; NRVMs subjected to "I/R"; and NRVMs pre-incubated with 3 μM 666-15 and subjected to I/R "I/R+6665-15." n = 4 independent cultures. (D) Representative traces and (E) average data of TG-induced Ca^{2+} influx in Fura-2 loaded NRVMs. Cells were

(legend continued on next page)

Please cite this article in press as: Falcón et al., Inhibition of adenylyl cyclase 8 prevents the upregulation of Orai1 channel, which improves cardiac function after myocardial infarction, Molecular Therapy (2024), https://doi.org/10.1016/j.ymthe.2024.01.026

SOCE involvement in the adverse cardiac remodeling has been proposed for several cardiomyopathies, including HF caused by AMI or by transaortic-induced overload, and right cardiac remodeling induced by pulmonary arterial hypertension, among other cardiac diseases.[5,7,8,23] Nevertheless, the contribution of SOCE to cardiac physiological Ca^{2+} homeostasis is considered limited, and the expression of Orai1 is rather low in the adult heart.[6] However, it is widely recognized that even slight alterations in Ca^{2+} signaling can gradually impact heart function, particularly when sustained over time.[24] Recent, compelling evidence demonstrated that Orai1 and other molecules players of SOCE are overexpressed during adverse cardiac remodeling.[7,25] In the current study, we demonstrated that I/R evokes significant upregulation of Orai1 days after the ischemic insult, consistent with other findings.[8,26] However, reports explaining how Orai1 is upregulated in such conditions are currently lacking. Here, we found that Orai1 overexpression potentiates SOCE in unstimulated cardiac cells and enhances diastolic $[Ca^{2+}]_i$, as demonstrated in field stimulated ARVMs and NRVMs. These findings are supported by the significant reduction in elevated diastolic $[Ca^{2+}]_i$ upon Orai1 inhibition using GSK-7975A and SYNTA66, two widely employed SOCE inhibitors.[20] Our findings are in line with a previous study demonstrating that Orai1 inhibition reduced aldosterone-induced diastolic $[Ca^{2+}]_i$ increase in NRVMs.[17] In addition to Orai1, other classical molecular players are known to participate in mishandling diastolic $[Ca^{2+}]_i$ in failing hearts, such as the hyperphosphorylation of RyR2 or the alteration of SERCA and Na^+/Ca^{2+} exchange activity, as reviewed recently.[24] Our current study determines a significant phosphorylation of RyR2 at Ser^{2030} in I/R heart tissue, which could facilitate Ca^{2+} leak and increase diastolic $[Ca^{2+}]_i$. This finding is consistent with a recent study in failing heart tissue from patients with ischemic cardiomyopathy, showing that phosphorylation of RyR2 increased sarcoplasmic reticulum Ca^{2+} leak.[27] Furthermore, the decay time constant of $[Ca^{2+}]_i$ transients is significantly increased in cardiac myocytes from I/R rats, indicating a slower rate of Ca^{2+} uptake by SERCA, which could contribute to the elevated diastolic $[Ca^{2+}]_i$ observed in I/R. Therefore, our data determine that at least two actors contribute to the increase of diastolic $[Ca^{2+}]_i$ under I/R, the activation of conventional RyR2 and Ca^{2+} influx through SOCE.

In addition to the upregulation of Orai1, we observed a significant increase in the expression of AC8 in I/R rat hearts. Independent studies demonstrated that AC8 interacts constitutively with the N-terminal site of Orai1, as demonstrated in various cells.[13–15] However, to the best of our knowledge, the connection between Orai1 and AC8 has not been investigated in cardiac myocytes. Herein, we found low but detectable co-localization in NRVMs and heart tissue under control condition. However, this co-localization increased acutely in NRVM subjected to a short period of I/R, indicating that the interaction between Orai1 and AC8 is dynamic and may depend on Orai1-dependent Ca^{2+} influx, as recently demonstrated in MDA-MB-231 breast cancer cell line.[13–15] Moreover, the co-localization of Orai1 and AC8 was enhanced in the hearts of I/R rats 1 week after the intervention, probably because both AC8 and Orai1 are overexpressed after the ischemic insult. Interestingly, the expression of Orai1 and AC8 are significantly increased in ventricle biopsies obtained from post-myocardial infarction patients with depressed LV ejection fraction (LVEF), as compared with non-HF donors, as in an I/R rat model.

Our results also demonstrate a functional interaction between both proteins, since we showed that I/R-induced Ca^{2+} entry through Orai1 activates AC8, which increases [cAMP]i, thus creating a point of convergence for Ca^{2+} and cAMP signals. These data agree with recent studies suggesting that SOCE selectively regulates cAMP synthesis by activating certain Ca^{2+} sensitive adenylyl cyclase variants (for reviews see[28,29]). Particularly, the activation of AC8 appears to require specific Ca^{2+} influx through SOCE,[13,14] because other channels as the arachidonic acid-regulated Ca^{2+}-selective channel and the diacylglycerol-activated transient receptor potential canonical channels have failed to induce AC8-mediated cAMP synthesis.[30,31] Although, a recent study suggested that AC8 can be activated by IP3-evoked Ca^{2+} release from junctional sarcoplasmic reticulum in cardiac atria and sinoatrial,[32] indicating that AC8 activation may not be limited to SOCE, at least in cardiac myocytes.

Recently, the interaction between Orai1α, the longer form of Orai1, and AC8 was described in HEK293 cells as responsible for spatially restricted crosstalk between Ca^{2+} and cAMP, and NFAT activation.[15] NFAT is a widely studied calcineurin substrate that regulates the transcription of many genes involved in the pathological remodeling in the heart.[33] In our study, we focused on CREB activation, as it is one of the well-studied targets of both Ca^{2+} and cAMP signaling in eukaryotic cells, such as neurons and vascular smooth muscle cells.[34,35] Our findings revealed that I/R stimulates phosphorylation of CREB, through cAMP activation of PKA. In addition, the expression of CREB was significantly increased in I/R rats 1 week after surgery, and trends to increase in biopsied ventricles of patients with ischemic HF, indicating that CREB is not only quickly activated by

pre-incubated with 2 μM TG in presence of 1 μM nifedipine to inhibit L-type Ca^{2+} channels. Recordings were from "Control" NRVMs, NRVMs subjected to "I/R," NRVMs pre-incubated with 3 μM 666-15 "I/R+666-15." n = 120–200 cells from 3–4 independent cultures. (F) Bar graph shows TG-induced *ORAI1*-promoter activation in A7r5 cell line measured by the relative luciferase activity expressed as the ratio of firefly/renilla activities and normalized to those of untreated A7r5 cells. Data are from untreated "Control" A7r5 cells, A7r5 exposed 5 min to 2 μM TG; cells pre-incubated with 3 μM 666-15 "TG+666-15"; or with 10 μM GSK-7975A "TG+GSK-7975A" before TG stimulation. n = 4–10 independent cultures. (G) Representative traces and (H) average data of TG-induced Ca^{2+} influx in Fura-2 loaded untreated NRVMs "control," NRVMs exposed to "I/R," and NRVMs transfected with siRNA of AC8 exposed to I/R, "I/R + siAC8." n = 150–300 cells from 3–5 independent cultures. (I) Immunoblots and summary data showing the expression of Orai1 in untreated NRVM "Control"; in NRVMs subjected to "I/R" and transfected with AAV9 holding mock plasmid; and in NRVMs transfected with AAV9-AC8, "I/R + AAV9-AC8." n = 4–6 independent cultures. I/R protocol corresponds with 3 h of ischemia and followed by 72 h of reperfusion in (C), (D), (E), and (G–I). Data are expressed as means ± SD. *, **, ***, and **** indicate significance at $p < 0.05$, $p < 0.01$, $p < 0.001$, and $p < 0.0001$, respectively.

Please cite this article in press as: Falcón et al., Inhibition of adenylyl cyclase 8 prevents the upregulation of Orai1 channel, which improves cardiac function after myocardial infarction, Molecular Therapy (2024), https://doi.org/10.1016/j.ymthe.2024.01.026

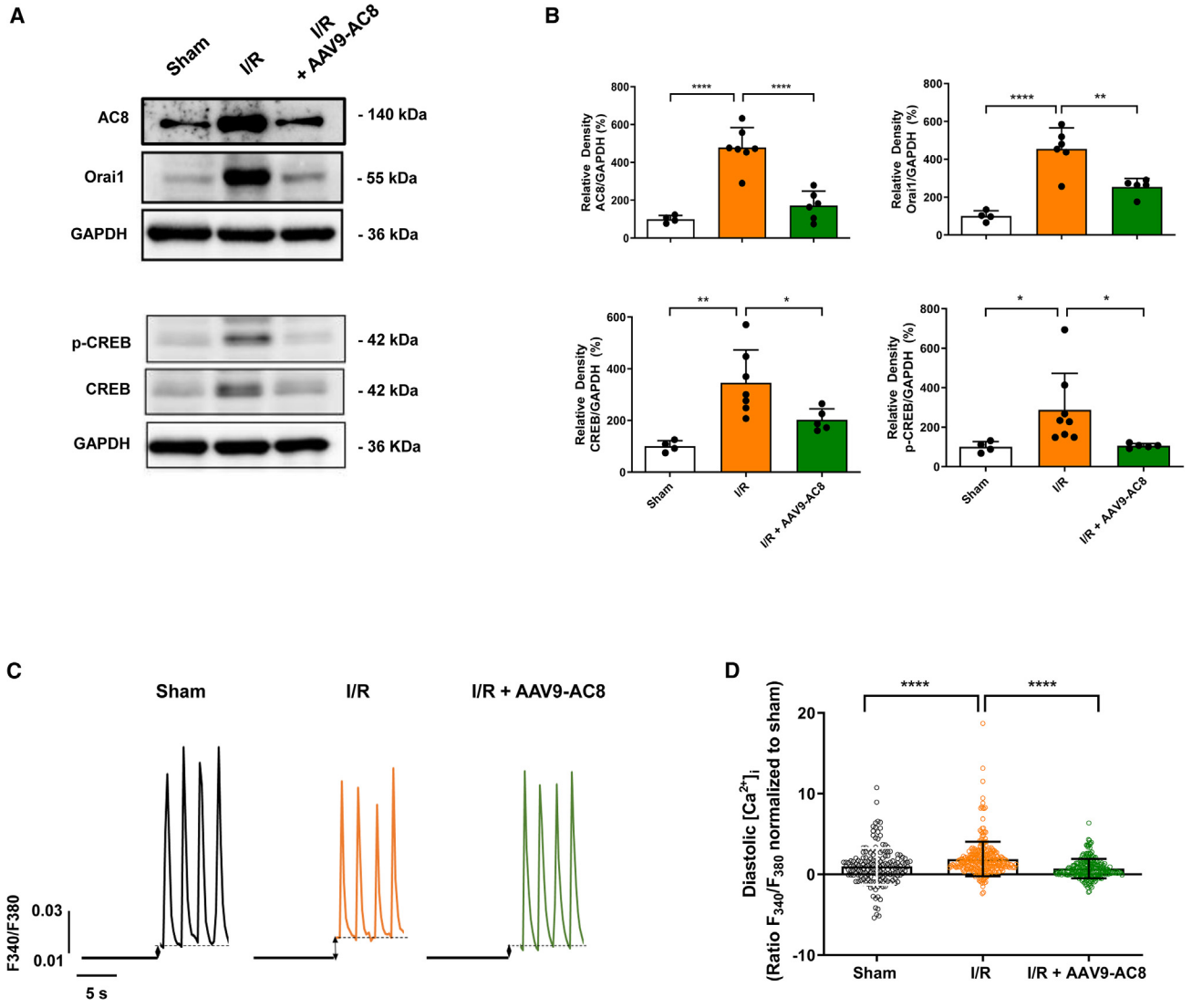

Figure 6. The intramyocardial administration of AAV9-AC8 prevents I/R-induced AC8, Orai1, *p*-CREB, and CREB upregulation

(A) Representative immunoblots and (B) summary data of AC8, Orai1, *p*-CREB, and CREB expression normalized to their corresponding GAPDH. Samples from heart tissue isolated from "sham"; "I/R" rats in which AAV9 holding mock plasmid was added by intramyocardial injection before reperfusion; and "I/R + AAV9-AC8" rats in which AAV9-AC8 was added by intramyocardial injection before reperfusion, were examined 1 week after surgery. n = 4–8 rats/condition. (C) Representative $[Ca^{2+}]_i$ transients (D) and summary data of diastolic $[Ca^{2+}]_i$ normalized to values in sham, recorded 1 week after surgery as Fura-2 ratio (F340/F380) in 0.5 Hz field stimulated cardiac myocyte dispersed 1 week after surgery from heart of "sham," "I/R" and "I/R + AAV9-AC8" rats. n = 170–240 cells from 4–5 rats/condition. Data are expressed as means ± SD. *, **, and **** indicate significance at $p < 0.05$, $p < 0.01$, and $p < 0.0001$, respectively.

I/R, but also it is overexpressed following ischemic insult, suggesting that CREB upregulation can play a role in promoting adverse cardiac remodeling and HF after AMI. As a transcription factor, CREB mediates gene transcription by binding to conserved cAMP-responsive elements in the promoter region of many genes.[36,37] Using different approaches, we provided evidence showing that CREB activation stimulated Orai1 transcription under I/R. In fact, blocking CREB with 666-15 specifically prevented I/R-induced Orai1 overexpression and the resulting exacerbation of SOCE. Furthermore, luciferase experiment demonstrated that a specific activation of *ORAI1* promoter by TG-induced SOCE in A7r5 cells was equally inhibited by SOCE inhibitor, GSK-7975A, and 666-15, confirming that CREB activation transcribes Orai1. Moreover, our results determined that AC8 is upstream of CREB activation by Orai1 because the suppression of AC8 elicited analogous inhibitory effects on the expression of Orai1 and the exacerbation of SOCE. Interestingly, the *in vivo* inhibition of the expression of AC8 by the intramyocardial administration of AAV9-AC8 significantly improved cardiac hemodynamic parameters, particularly global, circumferential, and radial strains, all of which are considered more sensitive indicators of cardiac fibers

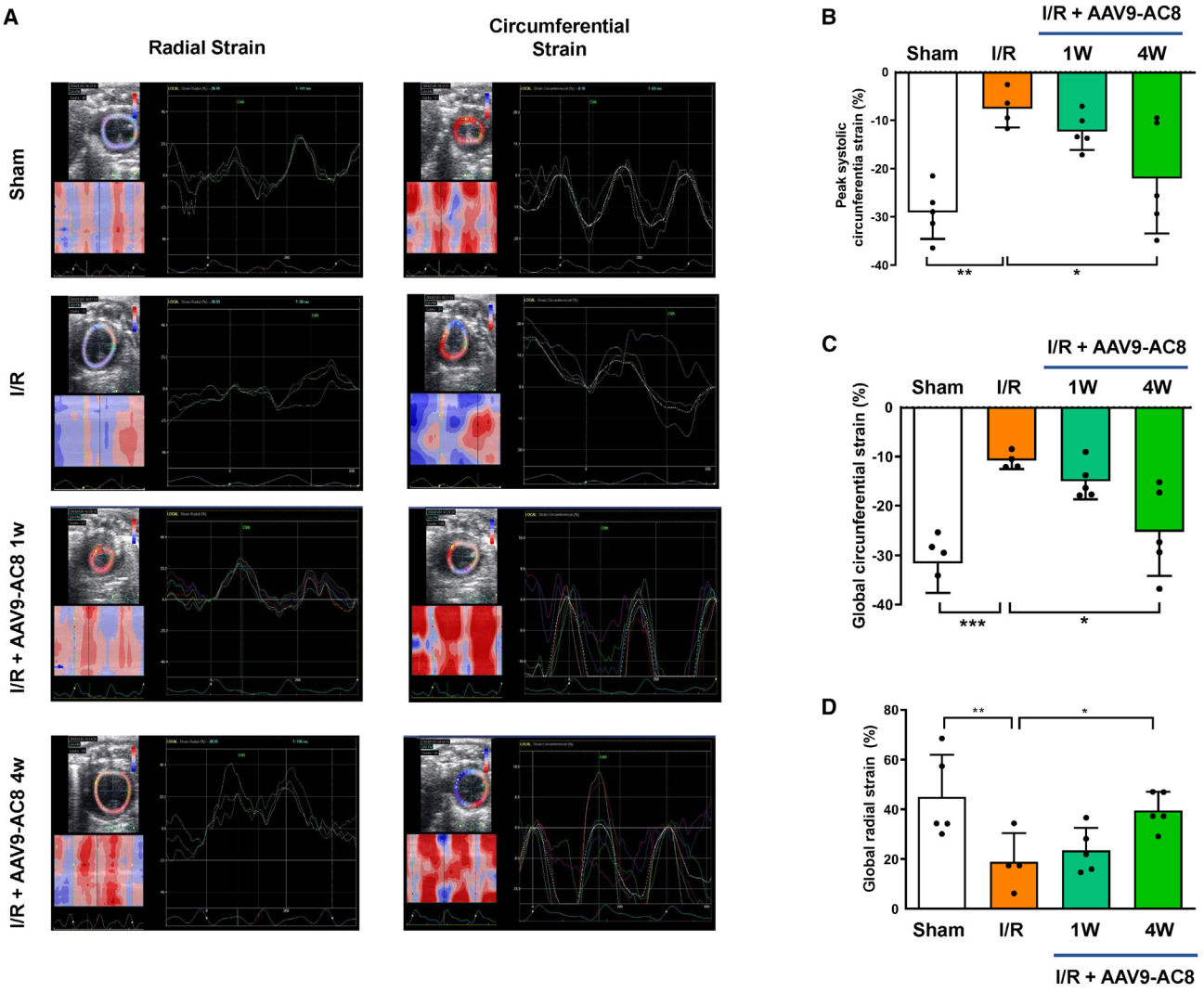

Figure 7. AAV9-AC8 improves hemodynamic parameters assessed by STE in I/R rats

(A) Representative images showing Radial strain (left) and circumferential strain (right) assessed by speckle tracking echocardiography (STE) in "sham," "I/R" rats in which AAV9 holding mock plasmid was added by intramyocardial injection, and "I/R" rats transfected with AAV9-AC8 examined 1 and 4 weeks after the intervention (I/R + AAV9-AC8 1W, I/R + AAV9-AC8 4W, respectively). (B–D) Graphs showing summary data presented in % of the PSCS (B), the GCS (C), and the GRS (D), in experimental group of rats as in (A). n = 4–5 rats/condition. Data are expressed as means ± SD. *, **, and *** and indicate significance at $p < 0.05$, $p < 0.01$, and $p < 0.001$, respectively.

deformation and dysfunction than the classical LVEF and LVFS evaluated by M-mode echocardiography.[38] These beneficial effects were accompanied with significant decreases in the expression of AC8, CREB and Orai1, and were associated with diastolic $[Ca^{2+}]_i$ recovery in stimulated adult cardiac myocytes. Currently, we lack an explanation for I/R-induced CREB overexpression and its inhibition caused by AC8 downregulation, which worth further investigation.

Altogether, our results propose a selective functional coupling between Orai1, AC8, and CREB in heart, which align with the accepted consensus on Ca^{2+}/cAMP signaling compartmentalization in membrane nanodomains, ensuring the specificity of cellular responses to restricted signaling molecules in subcellular regions of cardiac myocytes.[39,40] Previous studies suggest that overexpression of AC8 could precipitate and aggravate myocardial dysfunction,[41] or accelerate aging-related cardiac remodeling as proved in transgenic mice with specific cardiac overexpression of AC8 that demonstrated increased hypertrophy and fibrosis, ultimately leading to myocardial dysfunction and HF development.[42] By contrast, a recent study found that long-term elevation of AC8/cAMP/PKA/Ca^{2+} signaling in transgenic mice overexpressing AC8, resulted in complex adaptive responses that impacted heart structure and performance.[43]

Therefore, this study suggests that Ca^{2+} entry during I/R triggers a positive feedback loop formed by Orai1/AC8/CREB/Orai1, which compromises cardiac function and $[Ca^{2+}]_i$ handling. Therefore,

Please cite this article in press as: Falcón et al., Inhibition of adenylyl cyclase 8 prevents the upregulation of Orai1 channel, which improves cardiac function after myocardial infarction, Molecular Therapy (2024), https://doi.org/10.1016/j.ymthe.2024.01.026

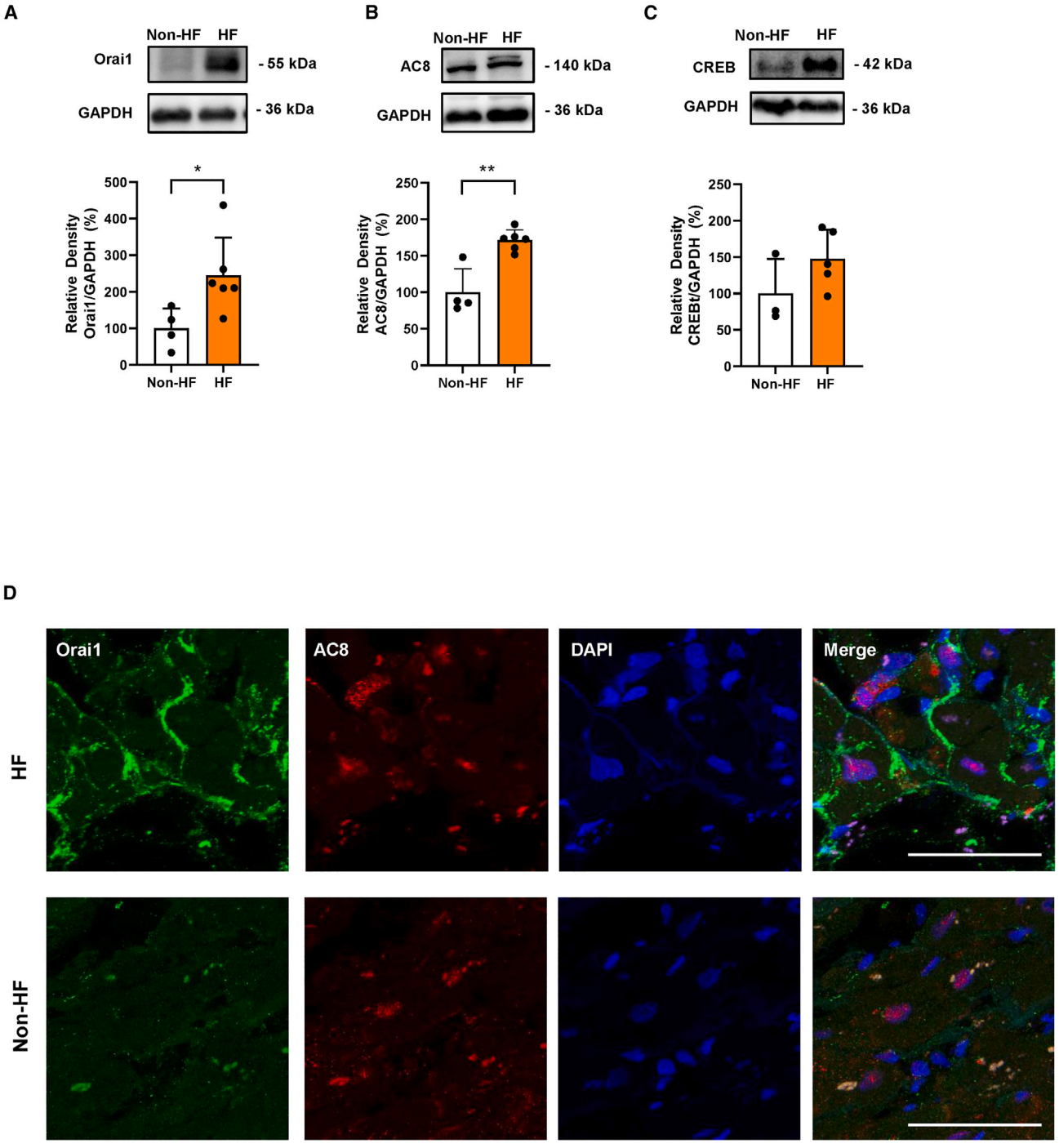

Figure 8. Expression of AC8, Orai1, and CREB in ventricle biopsies of ischemic patients failing hearts

Immunoblots and summary data showing the expression of Orai1 (A), AC8 (B), and CREB (C) normalized to their corresponding GAPDH. Samples were from left ventricle biopsies of ischemic patients with HF and from non-failing heart donors (non-HF). n = 4–6 biopsies/condition. (D) Representative images showing Orai1 (green), and AC8 (red) detected by immunofluorescence in a ventricle biopsy from ischemic failing (top) and non-failing hearts (bottom). Nuclei were stained with DAPI (Blue). Scale bar, 50 μm. Data are expressed as means ± SD. * and ** indicate significance at $p < 0.05$ and $p < 0.01$, respectively.

targeting the Orai1/AC8/CREB axis at the onset of I/R could present a new approach to limit the progression of the adverse cardiac remodeling toward HF in post-myocardial infarction patients.

MATERIALS AND METHODS

Study setting and approvals

This study was performed in accordance with the recommendations of the Royal Decree 53/2013 in agreement to the Directive 2010/63/EU of the European Parliament and approved by the local Ethics Committee on human Research of the University Hospital of Virgen del Rocio of Seville (Permission number: CEI 2013PI/096), and the Animal Research Committee of the University of Seville (Permission number: CI-00-2019).

Patients' myocardial biopsies

Left ventricle biopsies of ischemic patients with HF were obtained from 5 males and 3 females, with a median age of 62.9 ± 5.8 years old and LVEF = 26.8% ± 9.1%. These samples were obtained from patients undergoing surgery for cardiac transplantation at the University Hospital of Virgen del Rocio in Seville. Human biopsies were used for immunofluorescences and western blot approaches. We only analyzed biopsies with detectable staining or protein expression as confirmed with Ponceau staining. A signed informed written consent was provided from all donors. We also used ventricle biopsy from four healthy non-failing heart donors that were considered unsuitable for heart transplantation.

Rat model of myocardial I/R

Male Wistar rats (250 ± 50 g), aged 10–12 weeks, were anesthetized with intraperitoneal mixture of 50 mg/kg ketamine plus 8 mg/kg xylazine and maintained in 2% O_2/sevoflurane, as previously described.[44] Rats were ventilated with a tidal volume of 2.5 mL and 75–90 ventilations per minute (Harvard Apparatus). A left thoracotomy was performed in the intercostal space between the third and fourth ribs. The left coronary artery (LCA) was occluded with a 5-0 Prolene monofilament suture and a small PE-10 tube was placed in between for a convenient release upon reperfusion. LCA occlusion was confirmed by visual observation of cyanosis and ST-segment elevation monitored by continuous electrocardiogram (ECG). After 40 min of LCA ligation, reperfusion was initiated by releasing the knot and removing the tube, being confirmed by the appearance of epicardial hyperemic and ECG recovery. Analgesia was provided with meloxicam (1 mg/kg) for 3 days after surgery. Experiments were performed in the following experimental groups as illustrated in Figure S1A: "I/R" group: I/R produced by transient ligation of LCA; "sham" group: rats undergoing the same surgical procedure without coronary ligation; and the "I/R + AVV9-AC8" group: AVV9 holding AC8 shRNA mix was injected after ligation directly into the myocardium at 1×10^{11} vg/animal in a total volume of 150 μL. Animals were randomly subjected to LCA ligation with or without AAV9-AC8 infection. AAV9-AC8 serotypes (AAV9-AC8 A, B, and C) were acquired from GeneCopoeia. The company produces three AAV9 sequences that target AC8 to guarantee at least one of them with a minimum efficacy of 70%. The efficiency of AAV9-AC8 to decrease the expression of AC8 was tested in NRVMs using those serotypes as illustrated in the western blot shown in Figure S5. Based on this result, a proportional mix of AAV9-AC8 with sequences "B and C" was used in this study. Control experiments were conducted using AAV9 holding mock plasmid. All groups demonstrated a survival rate of 95%–100%.

Cardiac function analysis by echocardiography

Comprehensive echocardiographic studies were performed 1 and 4 weeks after surgery using the GE Vividi i ultrasound equipment, equipped with a 10 MHz transducer (General Electrics). Rats were anesthetized with 2% of sevoflurane to carry out the follow-up by echocardiography and experiments were performed with constant temperature. Images of the long and short axes were obtained at the level of the mitral valve, papillary muscles, and heart's apex. Parasternal longitudinal plane was used for analysis. The LVFS was calculated by the Teichholz and Simpson biplane methods. The speckle tracking echography analysis was performed using EchoPAC TM v110.1.2 software (GE Healthcare) as previously described.[45]

Isolation of rat ventricle myocytes

ARVMs were isolated from adult male heart of Wistar rats weighing 200–250 g by a Langendorff perfusion apparatus. ARVMs were isolated from left ventricle area of infarcted or sham heart, using collagenase type II (251 IU/mL; Worthington Biochemical), as previously described.[8] After perfusion, hearts were left in Petri dishes containing enzyme solution supplemented with 2 g/L BSA, and risk zone was gently stirred for 2–3 min at 37°C to disperse. Isolated cells were then filtered, centrifuged, and suspended in Tyrode solution containing (in mM) 130 NaCl, 1 $CaCl_2$, 0.5 $MgCl_2$, 5.4 KCl, 22 glucose, 25 HEPES, 0.4 NaH_2PO_4, and 5 $NaHCO_3$; pH 7.4. For stabilization, ARVMs were plated in a control solution containing 1.8 mM $CaCl_2$ at 37°C. For specific experiments cells were incubated with inhibitors before I/R experiments as shown in Figure S1B. I/R was performed using a simulated ischemic solution (in mM): 142 NaCl, 3.6 KCl, 1.2 $MgCl_2$, 1.8 $CaCl_2$, 5 $NaHCO_3$, 20 HEPES, 20 Lactate-Na, and 20 sucrose; pH 6.22, in a hypoxia chamber (1% O_2 and 5% CO_2), during 40 min. Reperfusion/reoxygenation started when the ischemic solution was removed and cardiomyocytes were returned to 21% O_2 and 5% CO_2 conditions. All experiments were performed on Ca^{2+}-tolerant rod-shaped myocytes.

For the isolation of NRVMs, hearts of 1- to 3-day-old Wistar rats were prepared using trypsin-DNAase (0.125%) as described previously.[44] NRVMs were grown in DMEM/M199 (4:1) supplemented with 10% horse serum, 5% fetal bovine serum (FBS), 1% glutamine, 100 U/ml penicillin, and 100 mg/mL streptomycin for 24 h, then medium was replaced and cells were incubated with inhibitors or AAV9-AC8 before I/R experiments, as illustrated in Figure S1C. In this case, NVRMs were incubated for 3 h in the ischemic solution. Reoxygenation/reperfusion was restored by removing the ischemic solution and placing NRVMs in an incubator at 21% O_2 and 5% CO_2 in DMEM/M199 (4:1) supplemented with 0.4% horse serum, 0.07% FBS, 100 U/mL penicillin and 100 μg/mL streptomycin.

Determination of the free intracellular calcium concentration ($[Ca^{2+}]_i$)

Transients of $[Ca^{2+}]_i$ were recorded in freshly isolated ARVM loaded with Fluo-3 AM by field stimulation using two parallel platinum electrodes, as described previously.[8] Confocal Ca^{2+} images were obtained with a 63× objective (w.i. and 1.2 N.A.) of Leica SP5 microscope by scanning cells with a white argon laser. Cells were excited at 500 nm and emission was collected at >510 nm in the line scan mode. The fluorescence values (F) were normalized by the basal fluorescence (F_0) to obtain the fluorescence ratio (F/F_0). Time constant of Ca^{2+} transient decay, the time from maximum liberation of Ca^{2+} during systole (F) to basal levels (F_0), was also analyzed.

For ratiometric experiments, ARVM and NRVM were loaded with Fura-2AM and performed using an inverted microscope Leica equipped with a 20× fluor objective (0.75 N.A.), a monochromator (Polychrome V, Till Photonics), and a light-sensitive CCD camera, controlled by HP software (Hamamatsu Photonics). $[Ca^{2+}]_i$ transients were recorded in a Ca^{2+} solution containing (in mM): 140 NaCl, 4 KCl, 1.1 MgCl2, 10 HEPES, 1.8 $CaCl_2$, and 10 glucose; pH = 7.4. SOCE experiments were conducted in NVRMs pretreated for 10 min with 2 μM TG and 1 μM nifedipine, inhibitor of L-type Ca^{2+} channel. To evaluate SOCE, experiments were carried out in free Ca^{2+} solution (in mM): 140 NaCl, 2.7 KCl, 4 MgCl2, 0.5 EGTA, and 10 HEPES (pH = 7.4), and Ca^{2+} influx was determined from changes in Fura-2 fluorescence after the re-addition of Ca^{2+} (2.5 mM). Changes in the $[Ca^{2+}]_i$ are represented as Δratio of Fura-2 AM fluorescence induced at an emission wavelength of 510 nm due to excitation at 340 and 380 nm (ratio = F340/F380) and calculated as the difference between the peak ratio after extracellular Ca^{2+} re-addition and its level right before.

Cell transfection

NRVMs were transfected with siRNA at 70% of confluence, 48 h after isolation, according to the manufacturer's instructions, using Lipofectamine RNAiMAX Transfection Reagent (Thermo Fisher Scientific). Cells were then maintained for another 24–48 h before performing experiments. Briefly, 5 μL lipofectamine was diluted in 150 μL Opti-MEM Medium, then 3 μL siOrai (10 μM) (Ambion, Thermo Fisher Scientific), and siRNA of AC8 (10 μM) (Merck-Sigma-Aldrich) was diluted in 150 μL of Opti-MEM Medium. Preparations were mixed in 1:1 proportion and incubated for 5 min at room temperature. NRVM were also infected with AVV9 holding AC8 shRNA (AAV9-AC8) using a multiplicity of infection of 2,000 to efficiently repress the expression of AC8.

Western blotting

Heart tissue was lysed using TissueLyser II (Qiagen) before adding protein lysis buffer. Protein samples from patients' biopsies, rat hearts and NVRMs were extracted using NP40 cell lysis buffer supplemented with inhibitor cocktail (Roche) and 1% of PMSF incubated for 30 min on ice. We subjected 40 μg samples of protein to SDS-PAGE (10% acrylamide, 6% for RyR2 WB) and electro-transferred to PVDF membranes. Membranes were blocked with 5% non-fat dry milk dissolved in Tris-buffered saline containing 0.1% Tween 20 (TTBS) for 2 h at room temperature (RT). Then, they were probed overnight at 4°C with primary antibodies anti-Orai1 (1:200, Abcam), *p*-CREB, and CREB (1:1000, Cell Signaling), anti-AC8 (1:1000, ProteinTech) for rat tissue, anti-AC8 (1:1000, Invitrogen) for human tissue, anti-*p*-RyR-Ser^{2030} (1:1,000, Badrilla), anti-RyR2 (1:1000, Santa Cruz), or anti-GAPDH (1:10000, GeneTex) in TTBS with 3% of BSA. After washing, membranes were incubated for 45 min at RT with horseradish peroxidase conjugated anti-IgG (Cell Signaling). Protein detection was performed on a ChemiDoc Touch (Bio-Rad), and images were analyzed using Image Lab software (Bio-Rad).

cAMP ELISA

The cAMP-Glo Assay (Promega) was used to measure cAMP production in homogenates from heart and isolated cardiomyocytes following the manufacturer's instructions. Luminescence was recorded on a GloMax 96 Microplate Luminometer (Promega). Isoproterenol, an agonist of beta-adrenergic receptors, was used as the positive control. cAMP levels are expressed as relative light units and normalized to the amount of protein.

Luciferase assay

The presence of several CREB response elements in the 5′-flanking region of the *ORAI1* gene promoter was determined by MatInspector software (Genomatix, GE). Luciferase assay was performed in A7r5 smooth muscle cell line. Sequence of 2989 kb of *ORAI1* gene promoter was synthesized and cloned in the pGL3-basic vector (Promega) upstream to firefly luciferase by Condalab. A7r5 cells were plated in 24-well plates at 2.5×10^4 cells/well in growth medium. The next day, cells were transfected with 500 ng/well of pGL3-Orai1 luciferase constructs and 25 ng the Renilla luciferase vector, pRL-TK (Promega) using DharmaFECT kb transfection reagent (Dharmacon) according to manufacturer's instructions. After 24 h, cells were pre-incubated with the CREB inhibitor, 666-15 (3 μM) or the Orai1 blocker, GSK-7975A (10 μM) for 3 h. Then, cells were treated with TG (2 μM). Twenty-four hours after treatment, luciferase activity was examined using Dual-Glo Luciferase Assay System. The activity test was performed and luminescence measured using a GloMax Discover Microplate Reader (Promega). Experiments were performed in duplicate and the luciferase activities were expressed as the relative Firefly/Renilla activities normalized to control.

Immunofluorescence

Samples from human and rat left ventricle were cleaned of blood in 1× PBS and quickly imbedded in optimal cutting temperature medium, then frozen in dry ice, and stored at −80°C. Samples were then cut in a cryostat and 6-μM sections were mounted on glass slides, fixed with formalin solution for 30 min, then stored at −20°C. After blocking with 1% BSA + 10% normal goat serum + 0.3% Triton X-100 for 1 h at RT, slides were incubated with an antibody against anti-Orai1 (1:100, Novus Biologicals) and anti-AC8 (1:200, Invitrogen) at 4°C overnight. Samples were then incubated with a species-specific secondary antibody conjugated to Alexa Fluor 488 goat anti-mouse-IgG and Alexa Fluor 594 goat anti-rabbit-IgG (1:250, Invitrogen) for

3 h and then with DAPI (0.1 mg/mL, Biorad), to visualize nuclei for 5 min at RT, gently washing with PBS between incubations. Finally, sections were washed again and coverslips were mounted in DAKO fluorescence mounting medium (DAKO), and were examined by a confocal microscope Leica TCS SP2 using a 63× objective with 2× zoom (Leica). Maximum intensity projections of all z-sections were performed (0.4 μm).

p-CREB immunofluorescence assays were performed in isolated AVRM and NRVM previously fixed with formalin solution for 20 min. Cells were incubated with rabbit anti-*p*-CREB primary antibody (1:200, Abcam) overnight and Alexa Fluor 488 goat anti-rabbit-IgG as secondary antibody (1:250, Invitrogen) in blocking solution for 2 h at RT. In NRVM, the cytoskeleton was stained with phalloidin-TRITC (1:100, Sigma-Aldrich). For ARVM we used anti-heavy chain cardiac myosin mouse primary antibody (1:400, Abcam, Cambridge, UK) and Alexa Fluor 594 goat anti-mouse-IgG as secondary antibody (1:250 dilution, Invitrogen). Images were visualized using a confocal microscope Leica TCS SP2. Maximum intensity projections of all z-sections were performed (0.4 μm for NRVMs and 0.8 μm for ARVMs) to measure *p*-CREB fluorescence in the nuclei. Mean fluorescence intensity of ROIs of the same area was analyzed using ImageJ software (NIH).

For Orai1 and AC8 co-localization studies, assays were performed in section of rat's heart and in NRVM using anti-Orai1 (1:100 Novus Biologicals) and anti-AC8 (1:200 ProteinTech). Images were visualized in the same z-position by Leica TCS SP2 confocal microscope using a 63× objective. PCC was analyzed randomly from 3 area of each picture and not limited to the infarcted are, using LasX software (Leica).

Statistical analysis

Data are presented as the mean ± SD. Analysis of statistical significance was performed with GraphPad Prism v.8.4.3 (GraphPad Software), using Shapiro-Wilk as normality test. For normally distributed variables we used the ordinary one-way ANOVA and performed multiples comparisons using t test without correction (Fisher's least significant difference test). We also used the Kruskal-Wallis non-parametric test with multiple comparisons corrected by Dunn's Test for non-normally distributed variables. For comparison between two groups, the Mann-Whitney U test (or Student t test for the analysis of Ca^{2+} determinations) was used. The outliers were removed based on results of QuickCalcs, an online tool of GraphPad. Throughout the manuscript *, **, *** and **** indicate p values of <0.05, <0.01, <0.001, and <0.0001, respectively.

DATA AND CODE AVAILABILITY

This study does not contain data that requires deposition in a public database. All data are available in the main text and the supplemental information.

SUPPLEMENTAL INFORMATION

Supplemental information can be found online at https://doi.org/10.1016/j.ymthe.2024.01.026.

ACKNOWLEDGMENTS

We wish to thank Professor José López Barneo, Dr. Maria Fernandez Velasco, and Dr. Abdelkrim Hmadcha for their critical reading of this manuscript; Dr. Gema Ruiz-Hurtado for offering RyR2 antibody; and Dr. María Caballero for her technical help with the echocardiography technique. Debora Falcon is the recipient of contract from PAIDI 2020 program financed by the European Social Fund and the Andalusian Government. This study was funded by Spanish "Agencia Estatal de Investigación" [PID2022-136279NB-C22/AEI/10.13039/501100011033]. This Research was also supported by grants [PID2022-136279NB-C21/AEI/10.13039/501100011033, and PID2019-104084GB/AEI/10.13039/501100011033]; "European Regional Development Fund; A way of making Europe," and by the "European Union" and The Andalusia Government [grants number: ProyExcel_00530; US-1381135].

AUTHOR CONTRIBUTIONS

D.F., E.C.-S., I.M.-G., M.M.-B., and A.D.-R. performed experiments, analyzed, and interpreted the data. A.O, J.A.R, and T.S. designed and supervised the experiments, analyzed, and interpreted the data. E.G.-C. and A.O. acquired clinical samples and data. D.F., E.C-.S., and J.A.R., drafted and reviewed the original paper. J.A.R. and T.S. acquired fundings and administrated the project. T.S. wrote and reviewed the paper.

DECLARATION OF INTERESTS

The authors declare that they have no competing interests.

REFERENCES

1. Yellon, D.M., and Hausenloy, D.J. (2007). Myocardial reperfusion injury. N. Engl. J. Med. *357*, 1121–1135. https://doi.org/10.1056/NEJMRA071667.

2. Ruiz-Meana, M., and García-Dorado, D. (2009). Translational cardiovascular medicine (II). Pathophysiology of ischemia-reperfusion injury: new therapeutic options for acute myocardial infarction. Rev. Esp. Cardiol. *62*, 199–209. https://doi.org/10.1016/S1885-5857(09)71538-5.

3. Falcón, D., Galeano-Otero, I., Martín-Bórnez, M., Fernández-Velasco, M., Gallardo-Castillo, I., Rosado, J.A., Ordóñez, A., and Smani, T. (2020). TRPC Channels: Dysregulation and Ca2+ Mishandling in Ischemic Heart Disease. Cells *9*. https://doi.org/10.3390/CELLS9010173.

4. Kho, C., Lee, A., and Hajjar, R.J. (2012). Altered sarcoplasmic reticulum calcium cycling–targets for heart failure therapy. Nat. Rev. Cardiol. *9*, 717–733. https://doi.org/10.1038/NRCARDIO.2012.145.

5. Bartoli, F., Bailey, M.A., Rode, B., Mateo, P., Antigny, F., Bedouet, K., Gerbaud, P., Gosain, R., Plante, J., Norman, K., et al. (2020). Orai1 channel inhibition preserves left ventricular systolic function and normal Ca2+ handling after pressure overload. Circulation *141*, 199–216. https://doi.org/10.1161/CIRCULATIONAHA.118.038891.

6. Avila-Medina, J., Mayoral-Gonzalez, I., Dominguez-Rodriguez, A., Gallardo-Castillo, I., Ribas, J., Ordoñez, A., Rosado, J.A., and Smani, T. (2018). The Complex Role of Store Operated Calcium Entry Pathways and Related Proteins in the Function of Cardiac, Skeletal and Vascular Smooth Muscle Cells. Front. Physiol. *9*, 257. https://doi.org/10.3389/FPHYS.2018.00257.

7. Masson, B., Le Ribeuz, H., Sabourin, J., Laubry, L., Woodhouse, E., Foster, R., Ruchon, Y., Dutheil, M., Boët, A., Ghigna, M.R., et al. (2022). Orai1 Inhibitors as Potential Treatments for Pulmonary Arterial Hypertension. Circ. Res. *131*, E102–E119. https://doi.org/10.1161/CIRCRESAHA.122.321041.

8. Domínguez-Rodríguez, A., Mayoral-Gonzalez, I., Avila-Medina, J., de Rojas-de Pedro, E.S., Calderón-Sánchez, E., Díaz, I., Hmadcha, A., Castellano, A., Rosado, J.A., Benitah, J.P., et al. (2018). Urocortin-2 Prevents Dysregulation of Ca2+

Homeostasis and Improves Early Cardiac Remodeling After Ischemia and Reperfusion. Front. Physiol. *9*, 813. https://doi.org/10.3389/FPHYS.2018.00813.

9. Nieto-Felipe, J., Macias-Diaz, A., Sanchez-Collado, J., Berna-Erro, A., Jardin, I., Salido, G.M., Lopez, J.J., and Rosado, J.A. (2023). Role of Orai-family channels in the activation and regulation of transcriptional activity. J. Cell. Physiol. *238*, 714–726. https://doi.org/10.1002/JCP.30971.

10. Makarewich, C.A., Zhang, H., Davis, J., Correll, R.N., Trappanese, D.M., Hoffman, N.E., Troupes, C.D., Berretta, R.M., Kubo, H., Madesh, M., et al. (2014). Transient receptor potential channels contribute to pathological structural and functional remodeling after myocardial infarction. Circ. Res. *115*, 567–580. https://doi.org/10.1161/CIRCRESAHA.115.303831.

11. Voelkers, M., Salz, M., Herzog, N., Frank, D., Dolatabadi, N., Frey, N., Gude, N., Friedrich, O., Koch, W.J., Katus, H.A., et al. (2010). Orai1 and Stim1 regulate normal and hypertrophic growth in cardiomyocytes. J. Mol. Cell. Cardiol. *48*, 1329–1334. https://doi.org/10.1016/J.YJMCC.2010.01.020.

12. Koga, Y., Tsurumaki, H., Aoki-Saito, H., Sato, M., Yatomi, M., Takehara, K., and Hisada, T. (2019). Roles of Cyclic AMP Response Element Binding Activation in the ERK1/2 and p38 MAPK Signalling Pathway in Central Nervous System, Cardiovascular System, Osteoclast Differentiation and Mucin and Cytokine Production. Int. J. Mol. Sci. *20*, 1346. https://doi.org/10.3390/IJMS20061346.

13. Willoughby, D., Everett, K.L., Halls, M.L., Pacheco, J., Skroblin, P., Vaca, L., Klussmann, E., and Cooper, D.M.F. (2012). Direct binding between Orai1 and AC8 mediates dynamic interplay between Ca2+ and cAMP signaling. Sci. Signal. *5*, ra29. https://doi.org/10.1126/SCISIGNAL.2002299.

14. Sanchez-Collado, J., Lopez, J.J., Jardin, I., Camello, P.J., Falcon, D., Regodon, S., Salido, G.M., Smani, T., and Rosado, J.A. (2019). Adenylyl Cyclase Type 8 Overexpression Impairs Phosphorylation-Dependent Orai1 Inactivation and Promotes Migration in MDA-MB-231 Breast Cancer Cells. Cancers (Basel) *11*, 1624. https://doi.org/10.3390/CANCERS11111624.

15. Zhang, X., Pathak, T., Yoast, R., Emrich, S., Xin, P., Nwokonko, R.M., Johnson, M., Wu, S., Delierneux, C., Gueguinou, M., et al. (2019). A calcium/cAMP signaling loop at the ORAI1 mouth drives channel inactivation to shape NFAT induction. Nat. Commun. *10*, 1971. https://doi.org/10.1038/S41467-019-09593-0.

16. Halls, M.L., and Cooper, D.M.F. (2017). Adenylyl cyclase signalling complexes - Pharmacological challenges and opportunities. Pharmacol. Ther. *172*, 171–180. https://doi.org/10.1016/J.PHARMTHERA.2017.01.001.

17. Sabourin, J., Bartoli, F., Antigny, F., Gomez, A.M., and Benitah, J.P. (2016). Transient Receptor Potential Canonical (TRPC)/Orai1-dependent Store-operated Ca2+ Channels: NEW TARGETS OF ALDOSTERONE IN CARDIOMYOCYTES. J. Biol. Chem. *291*, 13394–13409. https://doi.org/10.1074/JBC.M115.693911.

18. Correll, R.N., Goonasekera, S.A., van Berlo, J.H., Burr, A.R., Accornero, F., Zhang, H., Makarewich, C.A., York, A.J., Sargent, M.A., Chen, X., et al. (2015). STIM1 elevation in the heart results in aberrant Ca^{2+} handling and cardiomyopathy. J. Mol. Cell. Cardiol. *87*, 38–47. https://doi.org/10.1016/J.YJMCC.2015.07.032.

19. De Moudt, S., De Munck, D., Coornaert, I., and Fransen, P. (2021). GSK-7975A, an inhibitor of Ca2+ release-activated calcium channels, depresses isometric contraction of mouse aorta. Eur. J. Pharmacol. *906*, 174197. https://doi.org/10.1016/J.EJPHAR.2021.174197.

20. Shawer, H., Norman, K., Cheng, C.W., Foster, R., Beech, D.J., and Bailey, M.A. (2021). ORAI1 Ca2+ Channel as a Therapeutic Target in Pathological Vascular Remodelling. Front. Cell Dev. Biol. *9*, 653812. https://doi.org/10.3389/FCELL.2021.653812.

21. Mayr, B., and Montminy, M. (2001). Transcriptional regulation by the phosphorylation-dependent factor CREB. Nat. Rev. Mol. Cell Biol. *2*, 599–609. https://doi.org/10.1038/35085068.

22. Peng, J., Miller, M., Li, B.X., and Xiao, X. (2022). Design, Synthesis and Biological Evaluation of Prodrugs of 666-15 as Inhibitors of CREB-Mediated Gene Transcription. ACS Med. Chem. Lett. *13*, 388–395. https://doi.org/10.1021/ACSMEDCHEMLETT.1C00499.

23. Segin, S., Berlin, M., Richter, C., Flockerzi, R.M.V., Worley, P., Freichel, M., and Londoño, J.E.C. (2020). Cardiomyocyte-Specific Deletion of Orai1 Reveals Its Protective Role in Angiotensin-II-Induced Pathological Cardiac Remodeling. Cells *9*. https://doi.org/10.3390/CELLS9051092.

24. Val-Blasco, A., Gil-Fernández, M., Rueda, A., Pereira, L., Delgado, C., Smani, T., Ruiz Hurtado, G., and Fernández-Velasco, M. (2021). Ca2+ mishandling in heart failure: Potential targets. Acta Physiol. *232*, e13691. https://doi.org/10.1111/APHA.13691.

25. Sabourin, J., Boet, A., Rucker-Martin, C., Lambert, M., Gomez, A.M., Benitah, J.P., Perros, F., Humbert, M., and Antigny, F. (2018). Ca2+ handling remodeling and STIM1L/Orai1/TRPC1/TRPC4 upregulation in monocrotaline-induced right ventricular hypertrophy. J. Mol. Cell. Cardiol. *118*, 208–224. https://doi.org/10.1016/J.YJMCC.2018.04.003.

26. Gavali, J.T., Carrillo, E.D., García, M.C., and Sánchez, J.A. (2020). The mitochondrial K-ATP channel opener diazoxide upregulates STIM1 and Orai1 via ROS and the MAPK pathway in adult rat cardiomyocytes. Cell Biosci. *10*, 96. https://doi.org/10.1186/S13578-020-00460-W.

27. Walweel, K., Molenaar, P., Imtiaz, M.S., Denniss, A., dos Remedios, C., van Helden, D.F., Dulhunty, A.F., Laver, D.R., and Beard, N.A. (2017). Ryanodine receptor modification and regulation by intracellular Ca2+ and Mg2+ in healthy and failing human hearts. J. Mol. Cell. Cardiol. *104*, 53–62. https://doi.org/10.1016/J.YJMCC.2017.01.016.

28. Sanchez-Collado, J., Lopez, J.J., Jardin, I., Salido, G.M., and Rosado, J.A. (2021). Cross-Talk Between the Adenylyl Cyclase/cAMP Pathway and Ca2+ Homeostasis. Rev. Physiol. Biochem. Pharmacol. *179*, 73–116. https://doi.org/10.1007/112_2020_55.

29. Jardin, I., Berna-Erro, A., Nieto-Felipe, J., Macias, A., Sanchez-Collado, J., Lopez, J.J., Salido, G.M., and Rosado, J.A. (2022). Similarities and Differences between the Orai1 Variants: Orai1α and Orai1β. Int. J. Mol. Sci. *23*, 14568. https://doi.org/10.3390/IJMS232314568.

30. Shuttleworth, T.J., and Thompson, J.L. (1999). Discriminating between capacitative and arachidonate-activated Ca(2+) entry pathways in HEK293 cells. J. Biol. Chem. *274*, 31174–31178. https://doi.org/10.1074/JBC.274.44.31174.

31. Martin, A.C.L., and Cooper, D.M.F. (2006). Capacitative and 1-oleyl-2-acetyl-sn-glycerol-activated Ca(2+) entry distinguished using adenylyl cyclase type 8. Mol. Pharmacol. *70*, 769–777. https://doi.org/10.1124/MOL.106.025213.

32. Capel, R.A., Bose, S.J., Collins, T.P., Rajasundaram, S., Ayagama, T., Zaccolo, M., Burton, R.A.B., and Terrar, D.A. (2021). IP3-mediated Ca2+ release regulates atrial Ca2+ transients and pacemaker function by stimulation of adenylyl cyclases. Am. J. Physiol. Heart Circ. Physiol. *320*, H95–H107. https://doi.org/10.1152/AJPHEART.00380.2020.

33. Chaklader, M., and Rothermel, B.A. (2021). Calcineurin in the heart: New horizons for an old friend. Cell. Signal. *87*, 110134. https://doi.org/10.1016/J.CELLSIG.2021.110134.

34. Rodríguez-Moyano, M., Díaz, I., Dionisio, N., Zhang, X., Ávila-Medina, J., Calderón-Sánchez, E., Trebak, M., Rosado, J.A., Ordóñez, A., and Smani, T. (2013). Urotensin-II promotes vascular smooth muscle cell proliferation through store-operated calcium entry and EGFR transactivation. Cardiovasc. Res. *100*, 297–306. https://doi.org/10.1093/CVR/CVT196.

35. Parker, T., Wang, K.W., Manning, D., and Dart, C. (2019). Soluble adenylyl cyclase links Ca2+ entry to Ca2+/cAMP-response element binding protein (CREB) activation in vascular smooth muscle. Sci. Rep. *9*, 7317. https://doi.org/10.1038/S41598-019-43821-3.

36. Sands, W.A., and Palmer, T.M. (2008). Regulating gene transcription in response to cyclic AMP elevation. Cell. Signal. *20*, 460–466. https://doi.org/10.1016/J.CELLSIG.2007.10.005.

37. Kreusser, M.M., and Backs, J. (2014). Integrated mechanisms of CaMKII-dependent ventricular remodeling. Front. Pharmacol. *5*, 36. https://doi.org/10.3389/FPHAR.2014.00036.

38. Røe, Å.T., Ruud, M., Espe, E.K., Manfra, O., Longobardi, S., Aronsen, J.M., Nordén, E.S., Husebye, T., Kolstad, T.R.S., Cataliotti, A., et al. (2019). Regional diastolic dysfunction in post-infarction heart failure: role of local mechanical load and SERCA expression. Cardiovasc. Res. *115*, 752–764. https://doi.org/10.1093/CVR/CVY257.

39. Crul, T., and Maléth, J. (2021). Endoplasmic Reticulum-Plasma Membrane Contact Sites as an Organizing Principle for Compartmentalized Calcium and cAMP Signaling. Int. J. Mol. Sci. *22*, 4703. https://doi.org/10.3390/IJMS22094703.

40. Zaccolo, M., Zerio, A., and Lobo, M.J. (2021). Subcellular Organization of the cAMP Signaling Pathway. Pharmacol. Rev. *73*, 278–309. https://doi.org/10.1124/PHARMREV.120.000086.

41. Esposito, G., Perrino, C., Ozaki, T., Takaoka, H., Defer, N., Petretta, M.P., De Angelis, M.C., Mao, L., Hanoune, J., Rockman, H.A., and Chiariello, M. (2008). Increased myocardial contractility and enhanced exercise function in transgenic mice overexpressing either adenylyl cyclase 5 or 8. Basic Res. Cardiol. *103*, 22–30. https://doi.org/10.1007/S00395-007-0688-6.

42. Mougenot, N., Mika, D., Czibik, G., Marcos, E., Abid, S., Houssaini, A., Vallin, B., Guellich, A., Mehel, H., Sawaki, D., et al. (2019). Cardiac adenylyl cyclase overexpression precipitates and aggravates age-related myocardial dysfunction. Cardiovasc. Res. *115*, 1778–1790. https://doi.org/10.1093/CVR/CVY306.

43. Tarasov, K.V., Chakir, K., Riordon, D.R., Lyashkov, A.E., Ahmet, I., Perino, M.G., Silvester, A.J., Zhang, J., Wang, M., Lukyanenko, Y.O., et al. (2022). A remarkable adaptive paradigm of heart performance and protection emerges in response to marked cardiac-specific overexpression of ADCY8. Elife *11*, e80949. https://doi.org/10.7554/ELIFE.80949.

44. Mayoral-González, I., Calderón-Sánchez, E.M., Galeano-Otero, I., Martín-Bórnez, M., Gutiérrez-Carretero, E., Fernández-Velasco, M., Domenech, N., Crespo-Leiro, M.G., Gómez, A.M., Ordóñez-Fernández, A., et al. (2022). Cardiac protection induced by urocortin-2 enables the regulation of apoptosis and fibrosis after ischemia and reperfusion involving miR-29a modulation. Mol. Ther. Nucleic Acids *27*, 838–853. https://doi.org/10.1016/J.OMTN.2022.01.003.

45. Cerqueira, M.D., Weissman, N.J., Dilsizian, V., Jacobs, A.K., Kaul, S., Laskey, W.K., Pennell, D.J., Rumberger, J.A., Ryan, T., and Verani, M.S.; American Heart Association Writing Group on Myocardial Segmentation and Registration for Cardiac Imaging (2002). Standardized myocardial sementation and nomenclature for tomographic imaging of the heart: A Statement for Healthcare Professionals from the Cardiac Imaging Committee of the Council on Clinical Cardiology of the American Heart Association. Circulation *105*, 539–542. https://doi.org/10.1161/HC0402.102975.